USDA
United States Department of Agriculture

Physical Characteristics of Shrub and Conifer Fuels for Fire Behavior Models

Jonathan R. Gallacher, Thomas H. Fletcher, Victoria Lansinger, Sydney Hansen, Taylor Ellsworth, and David R. Weise

Forest Service
Pacific Southwest Research Station
Research Paper PSW-RP-269
March 2017

Authors

Jonathan R. Gallacher is a former graduate student and **Thomas H. Fletcher** is a professor, Department of Chemical Engineering, Brigham Young University, Provo, UT 84602; **Victoria Lansinger**, **Sydney Hansen**, and **Taylor Ellsworth** were students, Brigham Young University, Provo, UT 84602; **David R. Weise** is a research forester, U.S. Department of Agriculture, Forest Service, Pacific Southwest Research Station, 4955 Canyon Crest Drive, Riverside, CA 92507.

Cover photo: Horseshoe Meadows Hotshot firefighter (see back cover) takes a short breather at the Rim Fire on the Stanislaus National Forest in California, which began on August 17, 2013. U.S. Forest Service photo by Mike McMillan.

Abstract

Gallacher, Jonathan R.; Fletcher, Thomas H.; Lansinger, Victoria; Hansen, Sydney; Ellsworth, Taylor; Weise, David R. 2017. Physical characteristics of shrub and conifer fuels for fire behavior models. Res. Pap. PSW-RP-269. Albany, CA: U.S. Department of Agriculture, Forest Service, Pacific Southwest Research Station. 43 p.

The physical properties and dimensions of foliage are necessary inputs for some fire spread models. Currently, almost no data exist on these plant characteristics to fill this need. In this report, we measured the physical properties and dimensions of the foliage from 10 live shrub and conifer fuels throughout a 1-year period. We developed models to predict relative moisture content, apparent density, length, width, needle length, thickness, stem diameter, and surface area. Seasonal variability of the response variables was found to be adequately explained with a single model, so season-specific models or models with a seasonal parameter were unnecessary.

Keywords: Fuel element properties, live fuels, growth patterns, wildland fire, wildfire, *Adenostoma fasciculatum, Arctostaphylos glandulosa, Artemisia tridentata, Ceanothus crassifolius, Ilex glabra, Lyonia lucida, Pinus clausa, Pinus contorta, Pseudotsuga menziesii, Quercus gambelii.*

Summary

Fuels, weather, and topography influence wildland fire behavior. Thousands of vascular plant species in North America produce wildland fuels; however, the physical characteristics of only a small fraction of these species have been determined. As living organisms, vascular plants change dynamically over time on daily, monthly, seasonal, annual, and longer cycles. The physical characteristics of the living and dead plant components also change over time. The amount of water in a wildland fuel (moisture content) is perhaps the most widely measured and studied physical characteristic because of its importance for fire behavior and fire danger. Fire and fuel models typically assume that other physical characteristics remain constant. As part of a larger study of ignition of live foliage samples by radiant and convective heating, we measured the physical properties of foliage from 10 live shrub and conifer fuels throughout a 1-year period. A single model captured the effect of season on many of the physical characteristics. Linear regression produced a series of equations to predict relative moisture content, apparent density, length, width, needle length, thickness, stem diameter, and surface area of the foliage particles. The Weibull distribution modelled the dry mass of foliage particles enabling Monte Carlo simulation of the foliage component of the 10 shrub and conifer species for fire behavior simulation. This report presents the methodology and equations; the data reside in the Forest Service Research Data Archive (http://dx.doi.org/10.2737/RDS-2016-0023).

Contents

Introduction

Knowledge of the role of wildland fire in shaping the landscapes in North America has dramatically increased over the past 60 years. With this knowledge, federal wildland fire policy in the United States has evolved. The focus a century ago was on fire suppression. Current policy holds firefighter safety paramount while recognizing fire's important ecological functions as well as the economic impact that fire management has on the federal budget (Bunsenberg 2004, Fire Executive Council 2009, Stephens and Ruth 2005). A key component of the current policy is the emphasis on risk management and decision support, providing an impetus for the improvement of the current suite of operational fire models.

Models of wildland fire spread are of particular interest because they often form the basis of tactical and strategic responses to wildland fire events. Many fire spread models have been developed, each with various strengths and limitations. Fire models can be categorized in many ways. Two types of fire models, physics-based and empirical, following the definitions proposed by Weber (1991) and Sullivan (2009a, 2009b, 2009c), are described briefly herein. Examples of current physics-based models include FIRETEC and FDS along with its wildland-urban interface extension WFDS and WRF-Fire/CAWFE (Coen and Riggan 2014; Coen et al. 2013; Linn 1997; Linn and Cunningham 2005; Linn et al. 2005; McGrattan and Forney 2004; Mell et al. 2007, 2009). These models are based on fundamental physics and chemistry principles and solve the governing conservation equations in three-dimensional (3D) space. Although these models can provide useful insight into fire behavior, they are hampered by the lack of experimental data needed to validate the models and the resolution needed to model the fine-scale features of shrub and tree combustion (Clark et al. 2010, Sullivan 2009a). Examples of current empirical models used in the United States based on the Rothermel fire spread model (Albini 1976, Rothermel 1972) include BehavePlus, FIRECAST, FARSITE, and HFIRE (Cohen 1986, Finney 1998, Heinsch and Andrews 2010, Peterson et al. 2009). The Rothermel model was based heavily on experimentally derived fire behavior correlations to describe the underlying physics and chemistry of fire. Consequently, its predictions can be very accurate in some cases but inaccurate in others. The limitations of the Rothermel model as applied to live fuels are well-documented (Albini 1976, Cohen and Bradshaw 1986, Rothermel 1972) and have been demonstrated in chaparral fuel beds (Weise et al. 2016). Characterization of wildland fuels needed in current physics-based and empirical models is very limited (Weise and Wright 2014); a majority of the information has been incorporated into the Fuel Characteristics Classification System (Riccardi et al. 2007, USDA FS 2012). Solid fuel (i.e., grasses, shrubs, and trees) properties are modelled, and these models fall into three categories: allometric, 3D fuel placement, and fuel element property.

Allometric Models

Allometric models are single-stem models that can predict general fuel properties, such as fuel loading, canopy height, relative amounts of live and dead fuel, and biomass by size class. These models can be used in conjunction with remote sensing or ground cover data to describe general fuel properties over large areas. Considerable work has been done in this area. Most techniques are destructive and time-intensive (e.g., Brown 1976, 1978; Frandsen 1983; Helgerson et al. 1988; Ludwig et al. 1975; Riccardi et al. 2007; Schlecht and Affleck 2014; Williams 1989). The main drawback of these models, beyond the labor necessary to develop them, is their limited applicability—the regression equations are specific to both the fuel type and location. Efforts to improve these models and reduce the required labor through the use of remote sensing have received increased attention in recent years. Remote sensing data have been used to measure detailed information about individual plants and general information about large areas. Seielstad et al. (2011) found that remote sensing can be used to distinguish foliage and small branches from large branches in Douglas-fir.[1] Skowronski et al. (2007, 2011) and Barbier et al. (2012) discussed remote sensing models that predict properties such as canopy bulk density for large areas of land with a high degree of accuracy. A different approach is to use plant growth theory to predict bulk properties. One such model was developed by Bartelink (1998) and allows growth predictions to be adjusted based on simulated growing conditions. Although these models provide some necessary information to describe solid fuels, they do not provide all the necessary information. This is seen in the work by Wright (2013), in which prescribed burn plots with similar fuel loading and fuel type experienced widely different total burn areas even after accounting for weather variations.

Fuel Placement Models

Fuel placement models seek to capture the natural structure of plants and the resulting local fuel-density fluctuations. Research has shown fuel bulk density to be an important variable in fire propagation (Marino et al. 2012, Rothermel 1972, White and Zipperer 2010). Work by Parsons et al. (2011) illustrated the need for accurate 3D fuel characterization. Using a stochastic fuel placement technique called FUEL3D, they showed that, for the same mass and volume, fire spread behaves very differently between fuel beds with homogeneous fuel density and those with variable fuel density. Schwilk (2003) found that cutting dead fuel from the shrub canopy and placing it

[1] Spelling of scientific names of plants follows the PLANTS database (USDA NRCS 2016). With the exception of wax myrtle (*Morella cerifera* (L.) Small), scientific names mentioned in this report are listed in the tabulation on p. 6).

on the ground significantly reduced fire intensity, and thus concluded that canopy structure, not just fuel load, affects fire behavior. Weise and Wright (2014) cited several studies indicating the importance of fuel arrangement. Prince et al. (2014) developed a fuel placement model for chamise and juniper based on fractal theory (L-systems). They used bulk descriptors (Countryman and Philpot 1970) to provide guidance for the overall shrub properties, then built the shrub using the natural repeating patterns found in those species. Although these models provide the location in 3D space of the shrub's trunk, branches, and foliage, they do not provide a physical description of the various shrub parts that affect burning behavior (e.g., Loudermilk et al. 2009).

Fuel Element Property Models

Fuel element property models describe the physical, chemical, and shape properties of individual leaves or small branch segments. Chemical properties have received considerable attention (e.g., Behm et al. 2004, Hough 1969), but this work focuses on physical and shape properties, so chemical properties are not discussed further. Size, shape, and orientation of fine fuels could affect burning behavior (Lyons and Weber 1993). Fons (1946) found that properties like surface area, fuel volume, and foliage density are important in fire behavior predictions. More recent work (Engstrom et al. 2004, Fletcher et al. 2007, Shen 2013) showed fuel orientation and thickness can drastically influence ignition of shrub foliage. Despite the established effect of these physical properties and dimensions, there is a startling lack of data in the literature (Riccardi et al. 2007) on these characteristics. Countryman (1982) and Countryman and Philpot (1970) provided excellent descriptions of some common California shrub fuels, including fuel properties such as ash content, percentage of extractives, extractive heat content, density, surface area, and volume, but did not report other geometrical properties for the woody branches and foliage. Fahnestock and Key (1971) provided leaf measurements of wax myrtle. McNab et al. (1978) sampled a large number of southern pine stands with a palmetto-gallberry understory and developed regression equations to predict loading of different fuel bed components including live fuels <0.64 cm, but did not present other characteristics of the fuel particles. Hough and Albini (1978) presented other characteristics of the fuel particles; however, the basic dimensional measurements from this early work are no longer available.

Diameter, specific gravity, and surface-area-to-volume ratio for downed woody fuels from the branches of 19 western conifer species based on size class and age are available; foliage properties for these species were not determined (van Wagtendonk et al. 1996). Tree- and stand-level characteristics of crown fuels of western conifers including spatial variability and loading are available (Cruz et al. 2003, Keane et al. 2012, Reinhardt et al. 2006); no fuel particle properties were presented. Shen and Fletcher (2015) provided correlations for the geometrical properties of the foliage of four species to be used in fire spread models but did not measure surface area or density, two properties known to affect fire behavior. Pickett (2008) measured physical dimensions of several fuels but did not report any prediction models for these properties, although Prince (2014) reported correlations for manzanita leaves. We are aware of no other work that has been done to measure or model the physical properties and dimensions of individual fuel elements for live wildland fuels in the United States. This lack of data for individual live fuel particles also occurs elsewhere in shrub-dominated systems (e.g., Papió and Trabaud 1990, Pereira et al. 1995) and highlights the need to develop predictive models for other fuel types so that solid fuels can be characterized completely. This report presents measured dimensions and physical properties of foliage samples for 10 common plant species found in important fuel types in the United States (fig. 1) and the models developed from the measurements to predict these properties.

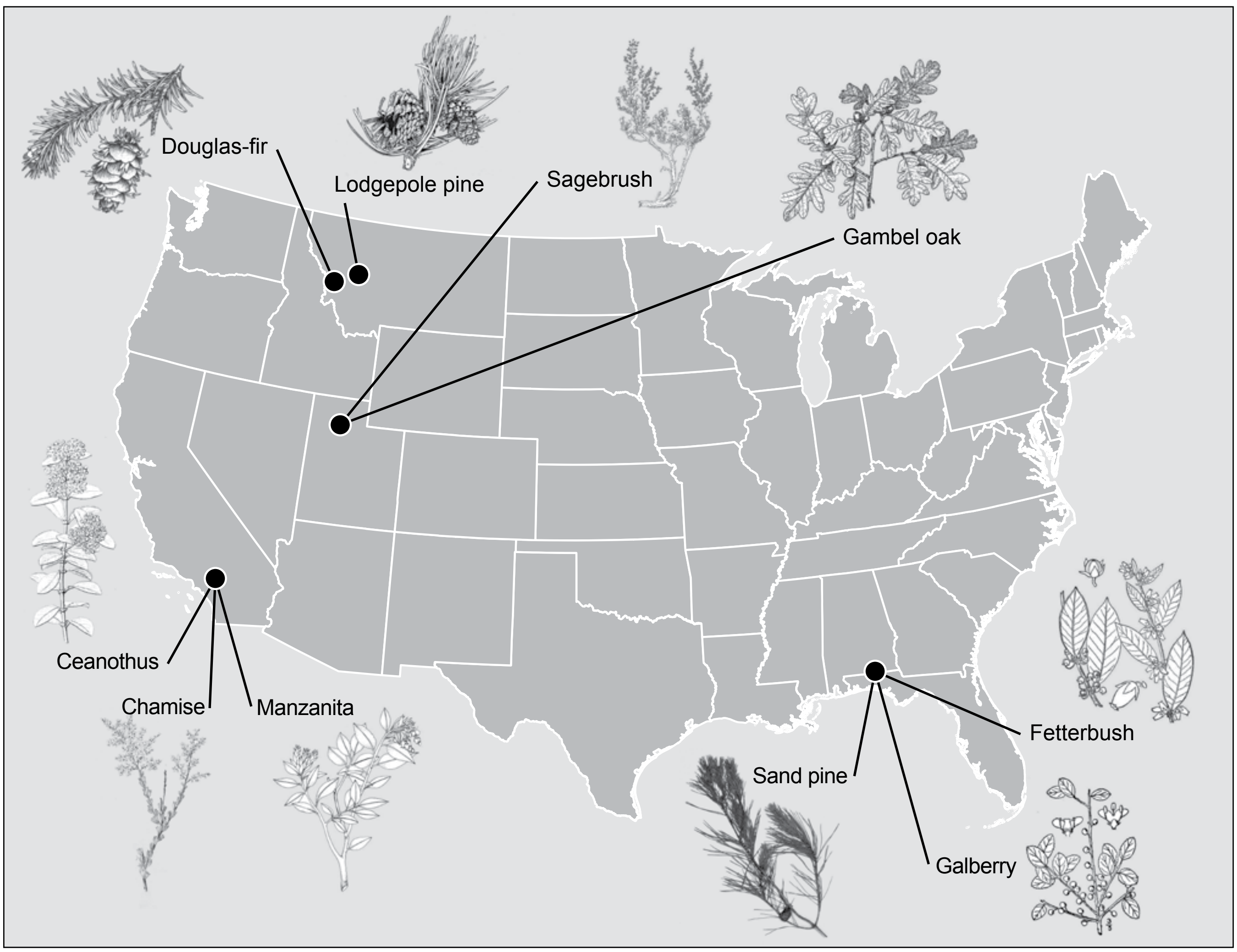

Figure 1—Sample collection locations and illustrations of 10 common plants found in important wildland fuel types in the conterminous United States. Images from Britton and Brown (1913), Conrad (1987), and Powell (2013).

Methods

As part of a project to determine the effects of radiant versus convective heating and live fuel moisture content on ignition of live fuels (Gallacher 2016; McAllister and Weise 2017; Weise et al. 2015; Yashwanth et al. 2015, 2016), physical properties of 10 plants common to important wildland fuel types were determined by measurement (see tabulation below and figure 1.) These data are available (Gallacher et al. 2016) for use. Various models were fit to the data to develop predictive models to be used in conjunction with 3D fuel placement models and allometric models to fully describe a shrub and provide the detail necessary for shrub combustion models (fig. 2).

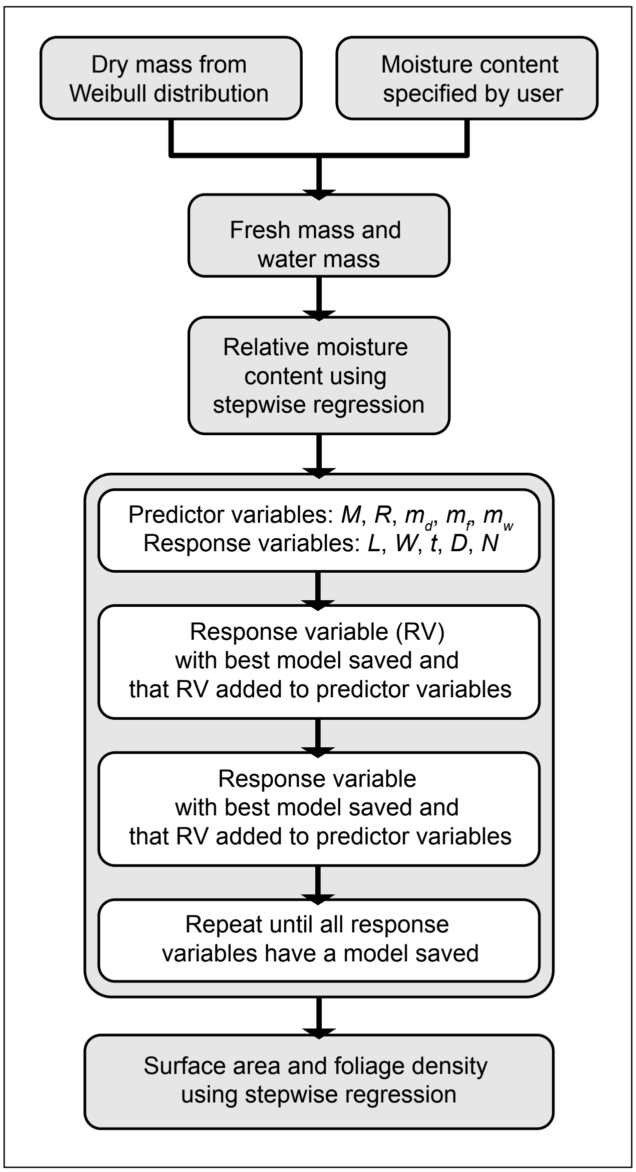

Figure 2—Flow chart for fuel element property model development. M = moisture content, R = relative moisture content, L = length, W = width, N = needle length, t = thickness, D = stem diameter, m_f = fresh mass, m_w = water mass, and m_d = dry mass.

Common name	Scientific name	Foliage
Chamise	*Adenostoma fasciculatum* Hook & Arn.	Needle
Douglas-fir	*Pseudotsuga menziesii* (Mirb.) Franco var. *glauca* (Beissn.) Franco	Needle
Big sagebrush	*Artemisia tridentata* Nutt.	Needle-like
Lodgepole pine	*Pinus contorta* Douglas ex Loudon var. *latifolia* Engelm. ex S. Watson	Needle
Sand pine	*Pinus clausa* (Chapm. ex Engelm.) Vasey ex Sarg.	Needle
Eastwood's manzanita	*Arctostaphylos glandulosa* Eastw.	Broadleaf
Hoaryleaf ceanothus	*Ceanothus crassifolius* Torr.	Broadleaf
Gambel oak	*Quercus gambelii* Nutt. var. *gambelii*	Broadleaf
Gallberry	*Ilex glabra* (L.) A. Gray	Broadleaf
Fetterbush	*Lyonia lucida* (Lam.) K. Koch	Broadleaf

Measurements

Physical dimensions, moisture content (MC), relative moisture content (RMC), and apparent density (ρ) were measured at the Brigham Young University Wildfire Lab in Provo, Utah, each month for 1 year. Typically, 25 replicates of each species were measured each month. All measurements were made within 48 hours of sample collection—nonlocal species were sealed in plastic bags and shipped overnight to Provo. The plastic bags were kept sealed and out of direct sunlight until measurements could be made. The 10 species were categorized as broadleaf or needle based on the shape of the foliage. Broadleaf samples consisted of whole, undamaged leaves while needle samples consisted of 2- to 6-cm branch tips with the foliage attached. Foliage samples were also categorized as new (current year) growth or old (prior year) growth:

Property	Definition
Length	Broadleaf: Distance from leaf base to leaf tip Needle, needle-like: Length of stem
Width	Broadleaf: Largest distance in direction perpendicular to length Needle, needle-like: Largest distance between needle tips normal to length
Thickness	Broadleaf: Distance from leaf top surface to bottom surface. Measured using calipers without crossing the main leaf vein
Needle length	Needle: Average length of sample
Stem diameter	Needle, needle-like: Diameter of stem holding needles
Mass	Mass of sample

Moisture content (dry basis, eq. 1) was estimated with a Computrac Max1000[2] moisture analyzer using a drying temperature of 95 °C; MC for live fuels ranges from 0 to 2.5 for many shrub species. Relative MC (Weatherley 1950) (eq. 2) was determined after soaking a sample in water for 24 to 48 hours before weighing to achieve full turgidity; RMC ranges from 0 to 1. Note that a calculation method using full turgid mass was proposed as an alternative method to determine specific gravity of small wood samples that eliminated the need to measure volume (Smith 1954). In the present study, several leaves or branch sections were necessary to reach the required minimum mass (1 g) so the reported MC and RMC are averages of several fuel particles.

$$\mathrm{MC} = \frac{m_f - m_d}{m_d} \tag{1}$$

$$\mathrm{RMC} = \frac{m_f - m_d}{m_t - m_d} \;, \tag{2}$$

where the mass subscripts *f*, *d*, and *t* denote fresh, dry, and turgid, respectively. Density was measured using Archimedes' principle that the force exerted on a submerged object is equal to the mass of the displaced fluid (Fernandes and Rego 1998, Ryan and Pickford 1978, Sackett 1980). Each sample was submerged in silicone oil (Dow Corning® 704 Diffusion Pump Fluid) and the weight of the displaced fluid was recorded. Using the density of the oil (1.07 g cm^{-3}), the volume of the sample was obtained. The presubmerged mass of the sample was used with the displaced volume to get the sample density. Oil was used instead of water to prevent the plant sample from absorbing the liquid into pores on the sample surface and to prevent fluid evaporation during mass measurements. Only whole leaves or needles were used, and three replicates were performed for each species each month. Aluminum 6061 rectangular blanks were used to verify the procedure. The density of aluminum 6061 is 2.72 g cm^{-3} (Narender et al. 2013). The estimated density of aluminum based on 10 samples with a 95-percent confidence interval was 2.72 ± 0.008 g cm^{-3}, indicating the validity of this approach to estimate density. Density was estimated for all species except chamise, big sagebrush, and lodgepole pine. Leaf external surface area for broadleaf species was obtained from images of each sample as has been done elsewhere (e.g., Weise et al. 2005). The surface area of one side of

[2] The use of trade or firm names in this publication is for reader information and does not imply endorsement by the U.S. Department of Agriculture of any product or service.

each leaf and the leaf perimeter were measured using in-house computer vision algorithms written in MATLAB (Gallacher 2016). The total surface area was then calculated (eq. 3), where A_s is the total external surface area, A_i is the area of the image, and P is the leaf perimeter.

$$A_s = 2A_i + PT. \tag{3}$$

Model Development

Before developing the property models, we determined if there were seasonal changes (Burgan and Susott 1991, Jolly et al. 2014, Philpot 1969, Weise et al. 2005) in the data using nonlinear mixed-effects models (Pinheiro and Bates 2000). Several functions of month were considered to model seasonal trends: no transformation, square, absolute value, power, sine and cosine. The significance of the seasonal term was determined by the F-statistic at a 99 percent significance level.

MC and m_d were the initial variables used to develop the prediction models (fig. 2). Dry mass was an input parameter for all the prediction models reported herein. We considered three two-parameter functions (beta, gamma, Weibull) to model dry mass frequency distribution. Forest growth and yield modelers frequently use the Weibull distribution to simulate distributions of biomass variables including the vertical distribution of foliage mass (e.g., Bailey and Dell 1973, Fleming 2001, Keyser and Smith 2010, Schreuder and Swank 1974). Other modelers prefer the beta distribution (Maguire and Bennett 1996). In the present study, the beta distribution could not be fit to three species when dry mass fell outside the interval [0, 1] even after scaling by the maximum observed value for the species. The gamma distribution generally performed slightly better than the Weibull distribution based on goodness of fit measures. However, the gamma parameter estimates were highly correlated (greater than 0.9) for all 10 species, and the Weibull estimates were not, so the Weibull distribution was selected to model dry mass of the fuel particles (eq. 4). In this report, we chose the *fitdist* routine of the *fitdistrplus* package (R Core Team 2013) because it is open-source software. The parameter estimates presented here differ from those reported in Gallacher (2016), which were estimated using the *wblfit* routine in Matlab®. Goodness of fit of the Weibull distribution was evaluated with three statistics—the Kolmogorov-Smirnov, Anderson-Darling, and Cramer-von Mises statistics and plots of the empirical and theoretical probability and cumulative distribution functions, quantile (Q-Q), and probability (P-P) plots. Because no single goodness of fit statistic captures characteristics of the entire function, visual assessment of the plots was favored (Delignette-Muller and Dutang 2015):

$$f\left(m_d;a,\ b\right)=\frac{b}{a}\left(\frac{m_d}{a}\right)^{b-1}\ e^{-\left(\frac{m_d}{a}\right)^b}$$
$$F\left(m_d;a,b\right)=1-e^{-\left(m_d/a\right)^b} \tag{4}$$
$$Q\left(p;a,b\right)=a\left(-\ln\left(1-p\right)\right)^{1/b}$$

where *f*, *F,* and *Q* are the probability density, cumulative distribution, and inverse cumulative distribution functions, respectively (Rinne 2008).

Predictive models were developed using the procedure shown in figure 2, which includes an iterative step. For each of the 10 species, several models were fit for each physical property using forward and backward stepwise regression. The best model for each property was selected using the adjusted R^2 value (Ezekiel 1930, Mason et al. 1989) and the Bayesian Information Criterion (BIC), (Burnham and Anderson 2004). From known MC and m_d, we calculated m_f and water mass $m_{H_20} = m_f - m_d$ by rearranging eq. 1. RMC was regressed against MC, m_f, m_d, and m_{H_20}; equations for the physical properties were developed simultaneously using RMC, MC, m_f, m_d, and m_{H_20}. The physical property response variable with the best fit was then added to the set of predictor variables, and the equations for the remaining physical properties were refit with the augmented set of predictor variables. This iterative process was repeated until equations for each of the physical properties were developed. Equations for A_s and ρ were fit via stepwise regression using all previously defined variables as predictor variables.

Property	**Unit**
MC, RMC	proportion
L, W, N	cm
T, D	mm
m_f, m_d, m_w	g
A_s	cm^2

Model Use

In addition to providing basic physical properties of the fuel particles used to interpret the results of the radiant/convective heating study, the equations we developed can be used in a predictive framework to simulate shrubs as in Parson et al. (2011) and Prince et al. (2014). The process to accomplish this is similar to the framework in figure 2. First, a value for desired MC is specified. The desired number of random values for the probability p is then generated (often generated from a uniform [0, 1] distribution), and the inverted cumulative distribution function (Q, eq. 4) generates the dry mass (m_d) using p and the estimated Weibull parameters ($\hat{a}$, $\hat{b}$) (Fishman 1997); m_f and m_w are then calculated using equation 1. The physical properties and RMC then follow from the several equations developed above.

Results and Discussion

Over the 2-year period of the study, 2,743 foliage and branch samples were measured (Gallacher et al. 2016). The number of fuel particles measured ranged from 150 for Gambel oak to 333 for chamise. Gambel oak is deciduous so its foliage was available for collection for only part of the year; similarly, access to the Douglas-fir and lodgepole pine sites was affected by snow.

Species	Count
Chamise	333
Douglas-fir	275
Big sagebrush	300
Lodgepole pine	220
Sand pine	290
Eastwood's manzanita	300
Hoaryleaf ceanothus	275
Gambel oak	150
Gallberry	300
Fetterbush	300

Water Content

Seasonal MC and RMC curves from the same region of the country exhibited similar but not identical behavior (fig. 3). California species had the lowest MC on average. Coniferous species (Douglas-fir, lodgepole pine, and sand pine) had consistently higher MC than other species from the same region. California and Rocky Mountain species had the lowest MC during the summer and fall months, and southern species experienced a maximum in MC during late summer. The lone deciduous species, Gambel oak, showed a strong relationship between MC and the growing season. Local fire seasons are nominally March through December in southern California (all year during drought years), May/June through October for the northern Rocky Mountains, and March through November for the southern coastal plain (Hull et al. 1966; Werth 2015a, 2015b). Moisture content is usually

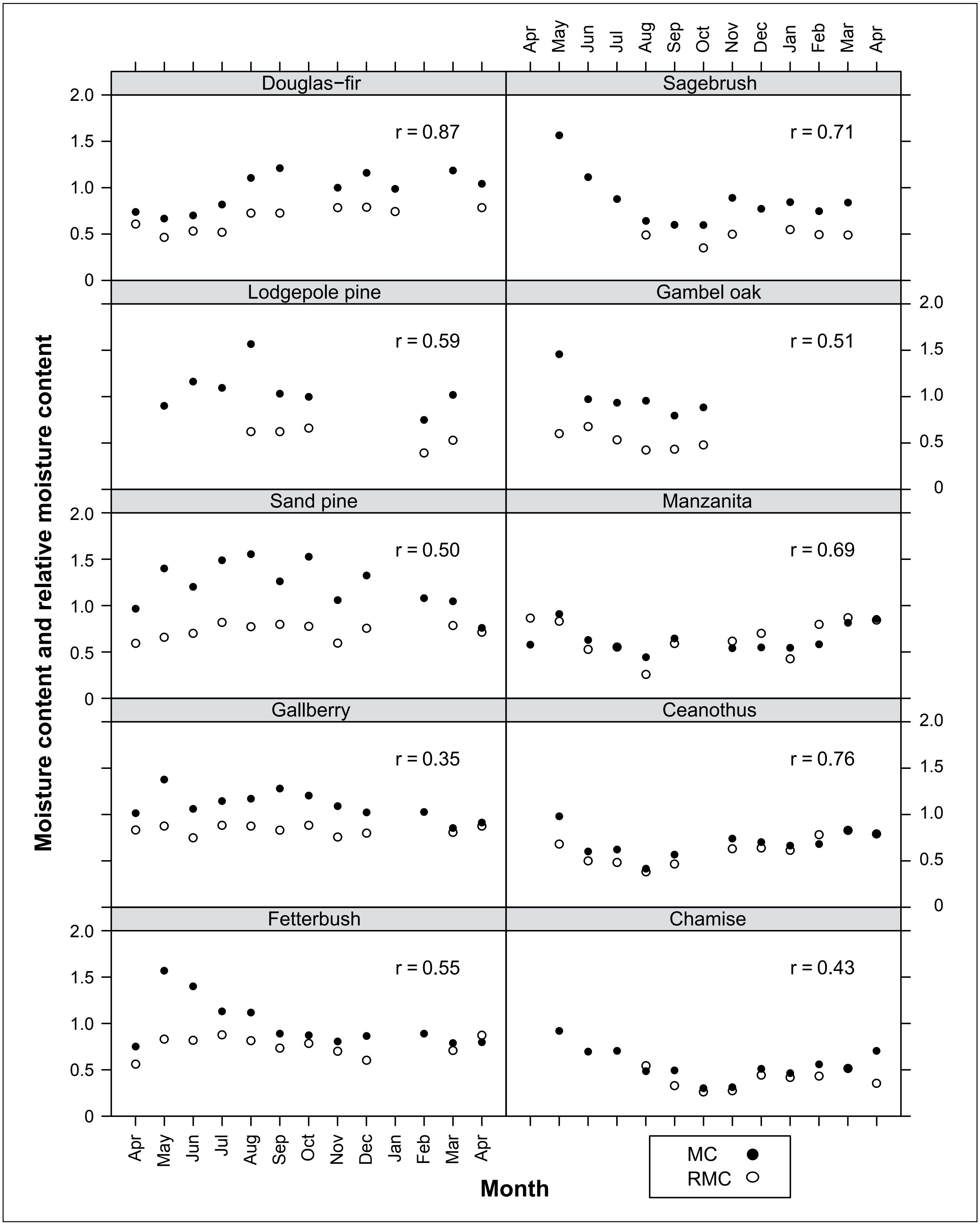

Figure 3—Yearly patterns for foliage moisture content (MC) and relative moisture content (RMC) for 10 live fuels from three regions of the United States.

lowest during the local fire season, although the agreement is far from perfect. The correlation between monthly mean MC and RMC was generally low (fig. 3); this is due in part to the small number of months. However, as in Jolly et al. (2014), we also found a statistically significant (probability of greater F-statistic $<1 \times 10^{-12}$) relationship between the water mass and the RMC (fig. 4). While our fitted model accounted for less of the variation (43 percent) in relative MC than Jolly's (2014) model (59 percent), the range of RMC in the present study (10 species) was greater (0.25 to 0.85 vs. 0.69 to 0.89) (1 species).

Only 13 percent of the nonmoisture sample characteristics exhibited seasonal changes. Summary statistics for the species characteristics that did not exhibit seasonal trends are in tables 1 and 2. If a particular characteristic exhibited a seasonal trend (such as the density of manzanita leaves), the figure illustrating the trend is identified in the table. Significant monthly trends for density (manzanita and Gambel oak), surface area (gallberry), thickness (fetterbush, Gambel oak, and manzanita), and width (gallberry) were observed (figs. 5 through 7). Surface area and width for gallberry both followed a similar trend and were correlated (fig. 5); large leaves were observed in April, small leaves in July, and relatively large leaves from August to the next April. The relatively high correlation between surface area and width is not surprising if the assumed leaf shape is elliptical; the surface area of an ellipse is a function of its major (length) and minor (width) axes ($A_S = \pi LW$). Density of manzanita was high in April, decreased rapidly to a low in August, and then increased slowly through March (fig. 6). Density for Gambel oak showed the opposite trend, with lows in May and October and a high in August. Thickness for fetterbush, Gambel oak, and manzanita all showed the same pattern: high in the spring, low in the summer, then increasing slowly through the rest of the sample period (fig. 7). Changes in density and thickness for manzanita compared to Gambel oak show some interesting relationships. Thickness and density for manzanita seemed to be correlated fairly well with each other ($R^2 = 0.76$), but the observed seasonal changes in thickness and density did not correlate solely to changes in MC ($R^2_{density} = 0.25$, $R^2_{thickness} = 0.12$). The trends for Gambel oak thickness and density were not well correlated ($R^2 = 0.10$). The trend for Gambel oak thickness is at least partly due to MC ($R^2 = 0.40$), while that for density had no relationship to MC ($R^2 = 0.00$).

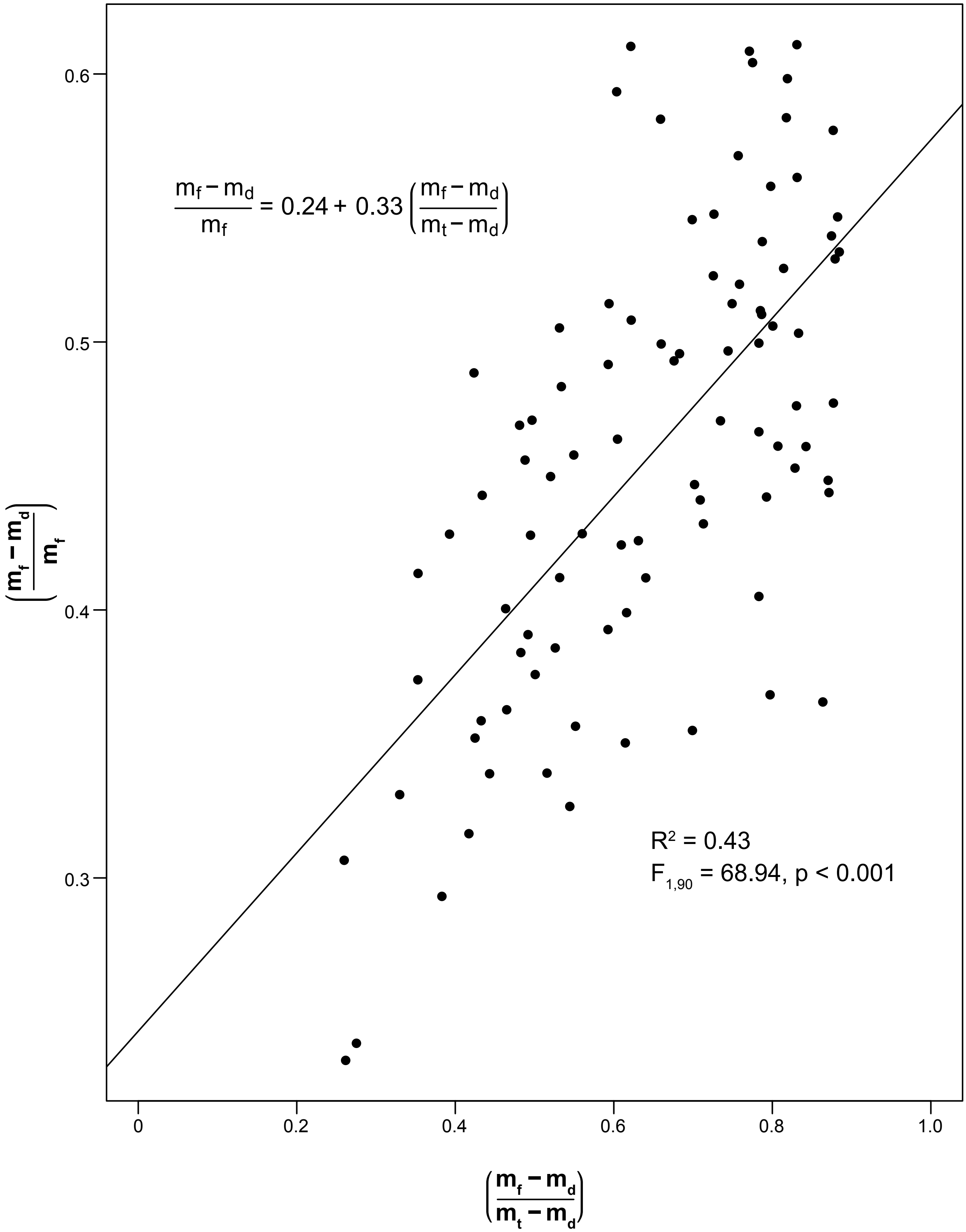

Figure 4—Relationship between water mass and relative moisture content for combined data from 10 different live fuels.

Table 1—Yearly mean and standard deviation for measured foliage characteristics—broadleaf species

Species	Density		Length		Width		Thickness		Surface area		Fresh mass	
	Grams per cubic centimeter		*- - - - - - - Centimeters- - - - - - -*				*- - Millimeters - -*		*Square - - centimeters - -*		*- - - Grams - - -*	
Manzanita	[a]		3.77	0.56	2.14	0.46	[b]		13.0	4.30	0.33	0.13
Ceanothus	0.99	0.03	1.60	0.28	1.23	0.23	0.57	0.11	3.2	0.97	0.09	0.04
Gambel oak	[a]		6.51	1.63	4.33	1.36	[b]		29.8	15.08	0.23	0.13
Fetterbush	0.89	0.04	5.25	1.06	2.51	0.63	[b]		19.2	8.01	0.28	0.12
Gallberry	0.89	0.03	3.89	0.73	[c]		0.32	0.06	[c]		0.12	0.05

Note: If the characteristic exhibited a significant seasonal trend, the figure that illustrates the trend is listed.
[a] See figure 6.
[b] See figure 7.
[c] See figure 5.

Table 2—Yearly mean and standard deviation for measured foliage characteristics—needle species

Species	Density		Length		Width		Needle length		Stem diameter		Fresh mass	
	Grams per cubic - - centimeter - -		*- - - - - - - - - - - - - Centimeters - - - - - - - - - - - - -*						*- - Millimeters - -*		*- - - Grams - - -*	
Douglas-fir	0.95	0.03	3.00	0.97	4.28	0.70	2.01	0.50	1.44	0.45	0.60	0.26
Lodgepole pine			2.24	0.45	8.57	2.45	5.44	0.97	3.14	1.00	1.33	0.47
Sand pine	0.98	0.03	2.47	0.92	7.02	2.35	5.60	1.09	1.35	0.41	0.67	0.25
Big sagebrush			4.42	0.47					1.22	0.39	0.22	0.13
Chamise			3.93	0.59			1.05	0.30	0.14	0.07		

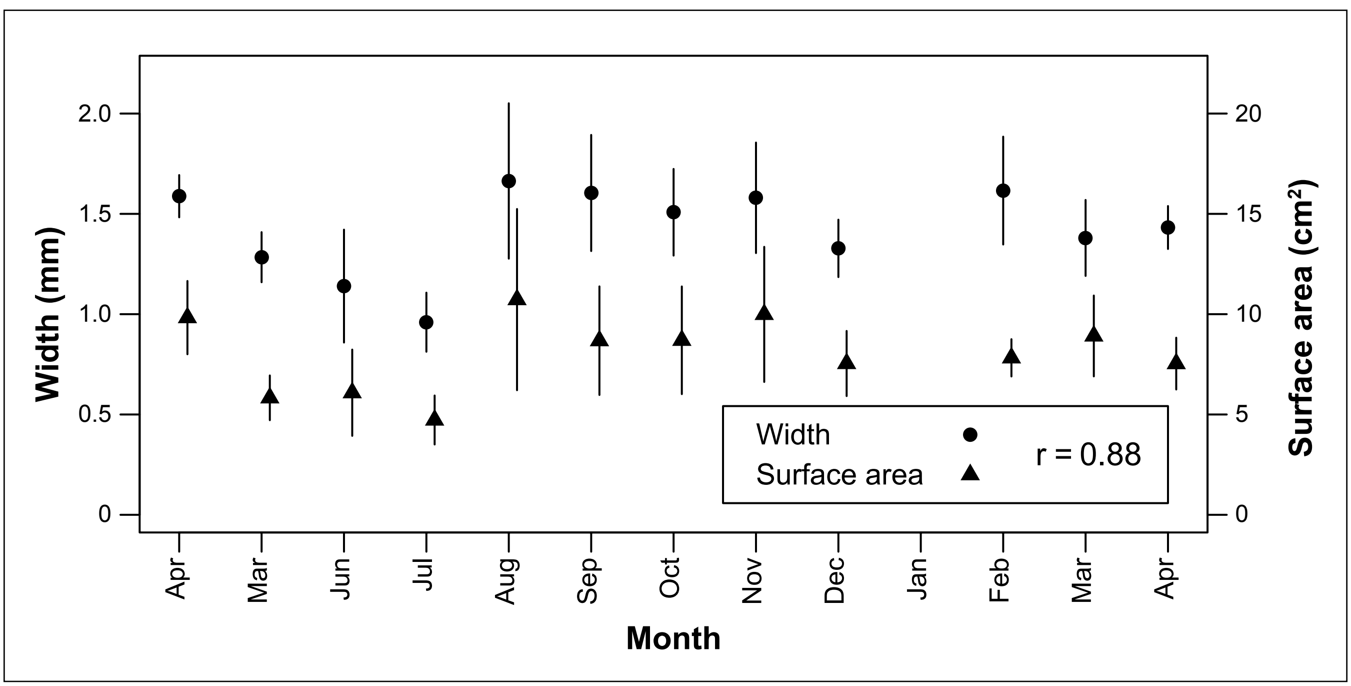

Figure 5—Monthly leaf surface area and width values for gallberry. Vertical lines indicate range of the mean ± the standard deviation. The month value is dithered to separate width and surface area data.

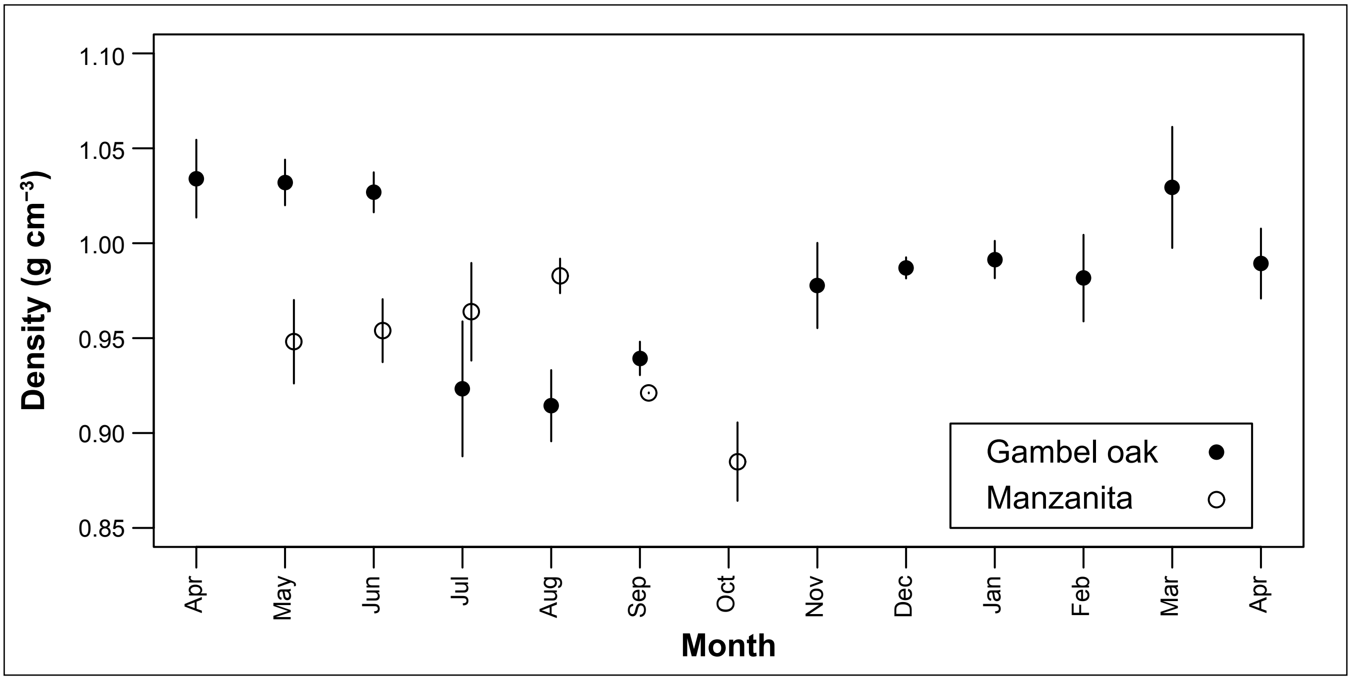

Figure 6—Monthly foliage density values for manzanita and Gambel oak. Vertical lines indicate range of the mean ± the standard deviation. The month value is dithered to separate species data.

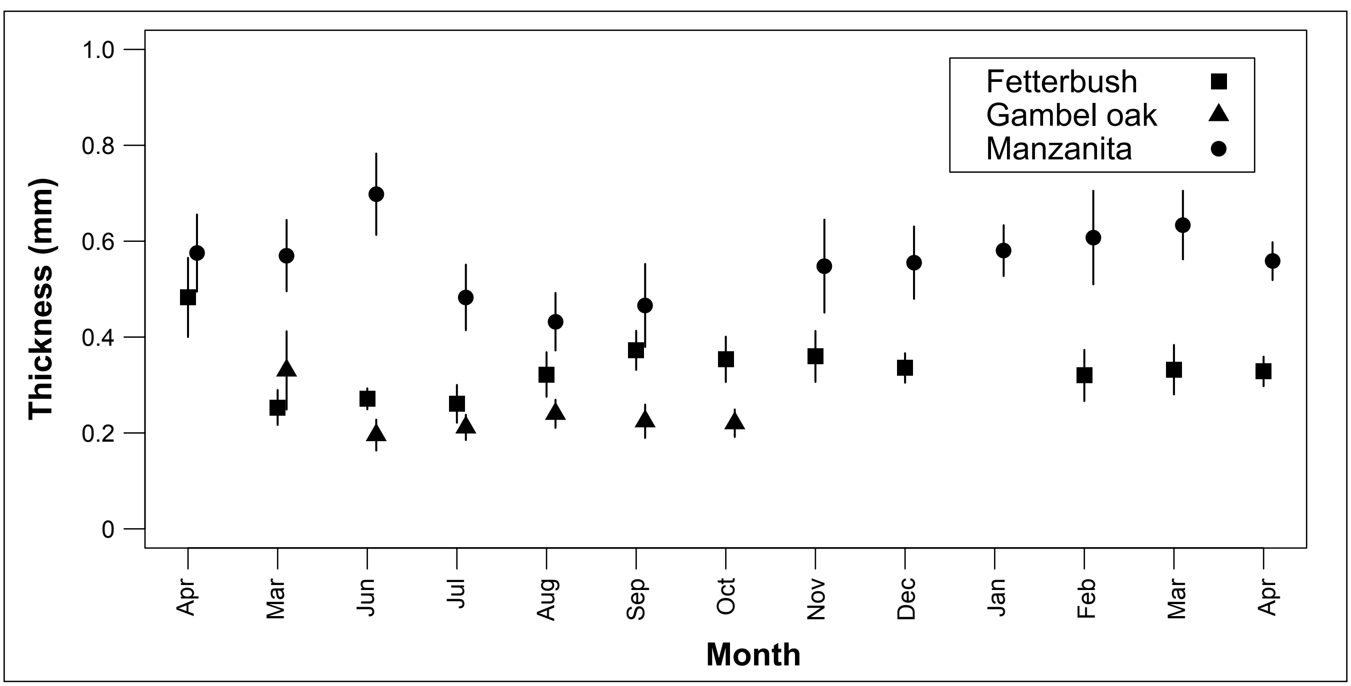

Figure 7—Monthly leaf thickness values for manzanita, Gambel oak, and fetterbush. Vertical lines indicate range of the mean ± the standard deviation. The month value is dithered to separate species data.

Mass Distribution

As can be seen in figure 8 and the appendix, the 2-parameter Weibull distribution fit a variety of empirical distributions of fuel particle mass. We separated the 10 species by the scale parameter ($\hat{a}$) into three groups. Estimates for the Weibull scale and shape parameters and the standard error of the estimates are contained in table 5 in the appendix. With the exception of lodgepole pine, the scale estimates were similar (appendix). There were no distinct seasonal trends in the mass data so the fitted distributions can be used throughout the year to simulate foliage mass. Although the data represent a random sample of the foliage within each species, caution should be used when applying these distributions. We assumed that the foliage/fuel particles did not change appreciably throughout the shrub or tree crown vertically. This assumption is valid for some species and not for others that have different leaf types in response to light. These are the first such measurements for some of these species.

Prediction Models

Regression models to predict four to six physical characteristics were developed. These prediction models for the various fuel element characteristics are shown in tables 3 and 4 for the broadleaf and needle species, respectively. The order of presentation in the table indicates the order in which they were developed and should be applied as they are interdependent per figure 2. The strength of each model is shown by the amount of data variation accounted for by the model as measured by R^2. For the overall collection of models, 36 percent have R^2 values greater than 0.7, and 72 percent have an R^2 value greater than 0.5. When broken out by species type, 50 percent of the broadleaf species models have an R^2 value greater than 0.7, and 90 percent have values greater than 0.5. Models for the needle species accounted for less of the data variation, with 17 and 48 percent of the models having an R^2 value greater than 0.7 and 0.5, respectively. The difference between needle and broadleaf species models in the amount of variation explained likely could have been reduced if the number of needles per sample was measured for the needle species. This was not practical. Many of the models suffer from severe multicollinearity. This issue is inherent in any dataset comparable to the one presented here owing to plant growth patterns and therefore cannot be avoided when trying to develop prediction models for foliage characteristics. However, the models can still be useful for prediction purposes as long as the relationships between measured characteristics in the model-development dataset are the same as the relationships between characteristics in the model-use dataset (Gujarati 2003).

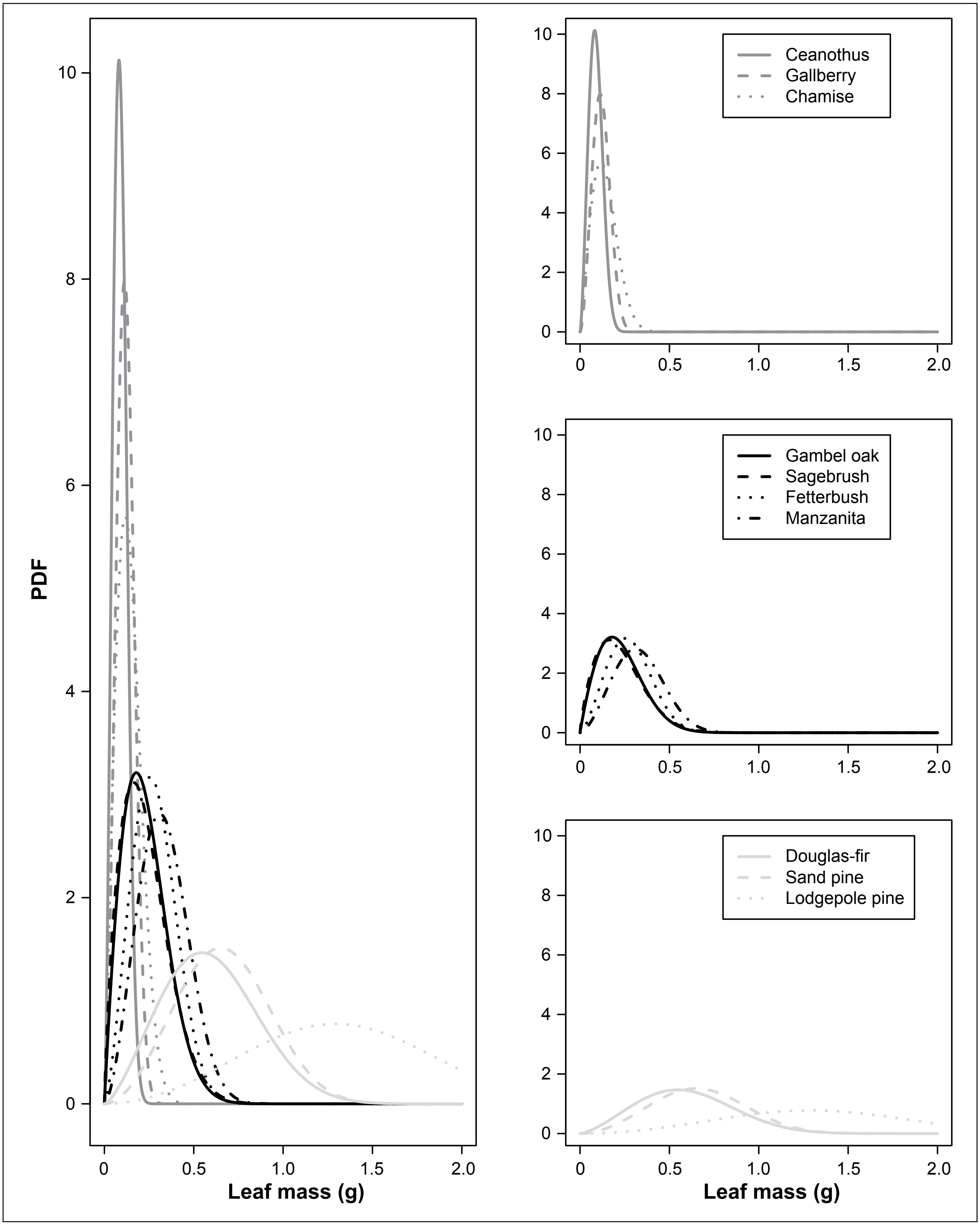

Figure 8—Fitted Weibull distributions for mass of foliage particles for 10 species of live fuels from the United States. All species are plotted on left graph; right graphs group species with similar scale ($\hat{a}$) parameters. PDF = probability density function.

Table 3—Regression equations developed to predict physical properties of foliage for several broadleaf species in the United States

Species and physical property	R^2_{adj}	Regression equation
Ceanothus:		
RMC	0.676	$0.568 + 32.11\sqrt{m_w} - 42.20\sqrt{m_f} + 28.28\sqrt{m_d}$
Length	0.615	$0.781 + 0.356\,(RMC)^2 - 0.494\ln(M) + 13.48m_w$
Width	0.523	$4.04 - 2.95\sqrt{m_w} + 0.703\ln(m_d) + 0.286\ln(RMC)$
Thickness	0.508	$0.671 - 38.42\sqrt{m_d} - 0.039L - 29.31\sqrt{m_w} - 0.499\sqrt{W} + 50.13\sqrt{m_f}$
Density	0.523	$1.28 - 0.124\ln(m_f) - 0.039\,(RMC)^2 - 0.096t^2 + 0.163\ln(m_w)$
SA	0.873	$-0.776 + 143.8m_d^2 + 1.35W + 1.14L$
Fetterbush:		
RMC	0.411	$4.41 + 2.94\ln(m_w) - 5.23 + 2.28\ln(m_d)$
Length	0.841	$8.67 + 0.656\ln(RMC) + 2.08\ln(m_d) + 0.935M^2$
Width	0.809	$82.15\sqrt{m_w} + 69.49\sqrt{m_d} - 102.1\sqrt{m_f}$
Thickness	0.662	$1.499 + 0.307\ln(m_f) - 0.298\ln(L) - 0.293\ln(W)$
Density	0.737	$0.626 - 0.793\ln(m_d) + 0.792\ln(m_f) - 0.198M^2 - 0.112\,(RMC)^2$
SA	0.948	$-4.92 + 20.09m_f^2 + 5.56W + 0.289L^2$
Gallberry:		
RMC	0.214	$-5.86 - 7.51\ln(m_w) + 7.57\ln(m_d) + M^2\left[6.69 - 6.05\ln(m_w) + 6.01\ln(m_d)\right]$
Width	0.740	$0.446 - 37.28m_d^2 + 0.174M^2 + 7.53m_f$
Length	0.714	$-8.503 + 4.165\ln(m_w) + 37.69\sqrt{m_d} - 7.03\ln(m_f)$
Thickness	0.597	$0.443 - 0.318\,(RMC)^2 + 0.623\sqrt{m_f} - 0.087\ln(L)$
Density	0.599	$1.393 - 8.89m_w^2 - 11.18m_d - 0.115M^2 + 6.17m_f - 0.455\sqrt{RMC}$
SA	0.905	$152.1m_w^2 - 2.40\,(RMC) + 1.54L + 1.60W^2$
Gambel oak:		
RMC	0.443	$133.3 - 438.5\sqrt{M} + 441.1\ln(m_f \quad m_d)$
Length	0.912	$4.073\,(RMC)^2 + 16.31\sqrt{m_d}$
Width	0.838	$9.388\sqrt{m_f}$
Thickness	0.720	$0.090 - 23.85\sqrt{m_d} + 32.22\sqrt{m_f} - 21.46\sqrt{m_w} - 0.088\ln(RMC)$
Density	0.879	$204.6 - 3.98\ln(m_w) - 695.6\ln(m_d) + 699.6\ln(m_f)$ $-0.199\,(RMC)^2 - 688.4\sqrt{M}$
SA	0.937	$60.4m_w + 0.371W^2 + 0.335L^2$

Table 3—Regression equations developed to predict physical properties of foliage for several broadleaf species in the United States (continued)

Species and physical property	R^2_{adj}	Regression equation
Manzanita:		
RMC	0.600	$-18.77 - 63.74 \ln(m_f) + 63.77 \ln(m_d) + 63.84\sqrt{M}$
Length	0.758	$1.232 + 4.48\sqrt{m_f}$
Width	0.631	$0.414 - 89.38\sqrt{m_w} - 0.264\,(RMC)^2 - 111.3\sqrt{m_d} + 145.8\sqrt{m_f}$
Thickness	0.619	$2.555 - 0.365\sqrt{L} - 0.296M + 0.398 \ln(m_w) - 0.338 \ln(W)$
Density	0.633	$0.858 + 0.0813\,(RMC)^2 + 0.817 m_w^2 + 0.215t - 0.1996 m_d$
SA	0.918	$-4.79 - 2.425 \ln(t) + 1.016W^2 + 12.51 m_f + 1.993L$

Note: R^2_{adj} is the adjusted R^2 value. The variables are relative moisture content (RMC), surface area (SA), moisture content (M), length (L), width (W), thickness (t), fresh mass (m_f), dry mass (m_d), and water mass (m_w).

Table 4—Regression equations developed to predict physical properties of foliage for several needle species in the United States

Species and physical property	R^2_{adj}	Regression equation
Chamise:		
RMC	0.631	$3.208 - 3.246M + 1.66 \ln(m_w \;\; m_d)$
Diameter	0.576	$1.039 - 1.50M^2 + 8.97 m_w$
Length	0.392	$-28.32 - 6.48 \ln(M) + 70.62 \ln(m_f) - \ln(m_d)\,[69.87 + 0.655 \ln(M)]$ $- (RMC)\,[32.00 + 45.13 \ln(M)]$
Douglas-fir:		
RMC	0.846	$-1.28 + 4.164 \ln(m_f) - 4.182 \ln(m_d) - 0.89M^2$
Length	0.723	$4.04 - 4.33\,(RMC)^2 + (29.32 - 20.78\sqrt{m_f})\,m_w^2$
NL	0.421	$[14.34 + 9.83 \ln(m_d)]\,\sqrt{R} - [9.05 + 7.47 \ln(m_d)]\,\sqrt{M}$
Width	0.524	$1.564 m_w + 1.15\,(NL) + [2.94 - 0.748 \ln(L)]\,(RMC)$
Diameter	0.418	$-1.14 \ln(m_f) + W^2\,(0.176 - 0.261\sqrt{m_d}) - (NL)\,(2.435 - 4.49\sqrt{m_d})$
Density	0.303	$-1.06 + 1.13\sqrt{M} + 0.16 \ln(RMC) + 1.30 \ln(m_f) - 1.32 \ln(m_w)$
Lodgepole pine:		
RMC	0.773	$5.89 + 7.62 \ln(m_w \;\; m_f) - 3.36 \ln(M)$
Diameter	0.614	$34945\sqrt{m_f} - [2719 - 999.6\,(RMC)^2]\,\sqrt{m_d} - [2218 + 1004\,(RMC)^2]\,\sqrt{m_w}$
Length	0.524	$4.24 - 1.55M^2 + 1.05\sqrt{m_w} - 0.856\sqrt{D} + (3.92M^2 - 4.22)\,(RMC)^2$

Table 4—Regression equations developed to predict physical properties of foliage for several needle species in the United States (continued)

Species and physical property	R^2_{adj}	Regression equation
NL	0.45	$-248.8 + 383.4 \ln (m_f) - 374.8 \ln (m_d) - [13.35 + 268.7 \ln (M) + 9.52 \ln (m_d)] \sqrt{RMC}$
Width	0.31	$[94.56 + 47.66M + 151.2 \ln (m_d) - 205.1 \ln (m_f) + 0.0073L^2 + 53.81 \ln (m_w)]^{-1}$
Sagebrush:		
RMC	0.821	$-46.96 + 158.8 \ln (m_d \quad m_f) + 157.4\sqrt{M}$
Diameter	0.493	$-0.811M^2 + 4.35 \ln (m_f) - 4.004 \ln (m_d)$
Length	0.493	$5.78\sqrt{RMC} - (2334 + 2452M^2)\sqrt{m_w} + (1213 + 3563M^2)\sqrt{m_d}$
Sand pine:		
RMC	0.24	$0.738 + 4.650m_w^2 - 2.264m_f^2 + 4.083m_d^2$
Length	0.634	$5.26 - M^2(3.58 - 1.143\sqrt{m_w}) + \ln (RMC)(12.22 + 11.42M^2)$
Width	0.355	$9.11 - 4.37 \ln (L) + 5.09m_f^2 - 11.78\,(RMC)\,m_w^2$
NL	0.481	$6.34 + 1.57M^2 - 6.84 \ln (m_f) + 1.89 \ln (W) + 8.02 \ln (m_d)$
Diameter	0.224	$41.46 - 3.144\sqrt{L} - 33.16\sqrt{M} - (42.07 - 38.44\sqrt{M})\sqrt{RMC}$ $-(2.37 - 1.850\sqrt{L})\sqrt{NL}$
Density	0.571	$0.841 - 0.0675 \ln (M) - 0.0014L^2 - 0.0011W + 0.202\sqrt{RMC}$

Note: R^2_{adj} is the adjusted R^2 value. The variables are relative moisture content (RMC), needle length (NL), moisture content (M), length (L), width (W), diameter of stem (D), fresh mass (m_f), dry mass (md), and water mass (m_w).

None of the models developed here contain a seasonal parameter. Although this lack of a seasonal parameter is not typical for plant growth models, the constancy of the measured data throughout the year made the inclusion of a seasonal parameter unnecessary. The measured characteristics that did change with season changed in concert with other characteristics (usually MC) so that the single prediction model is valid for the whole year. Although some of the needle species, particularly sand pine, exhibited visual seasonal variation in the shape and size of individual fuel samples, the statistical test for seasonal trends did not detect this. The variability in the sand pine data rendered differences based on growing season indistinguishable from the general trends. To illustrate the range of variability associated with the fitted models, three plots illustrating high (0.95), moderate (0.49), and low (0.24) R^2 values are shown in figure 9.

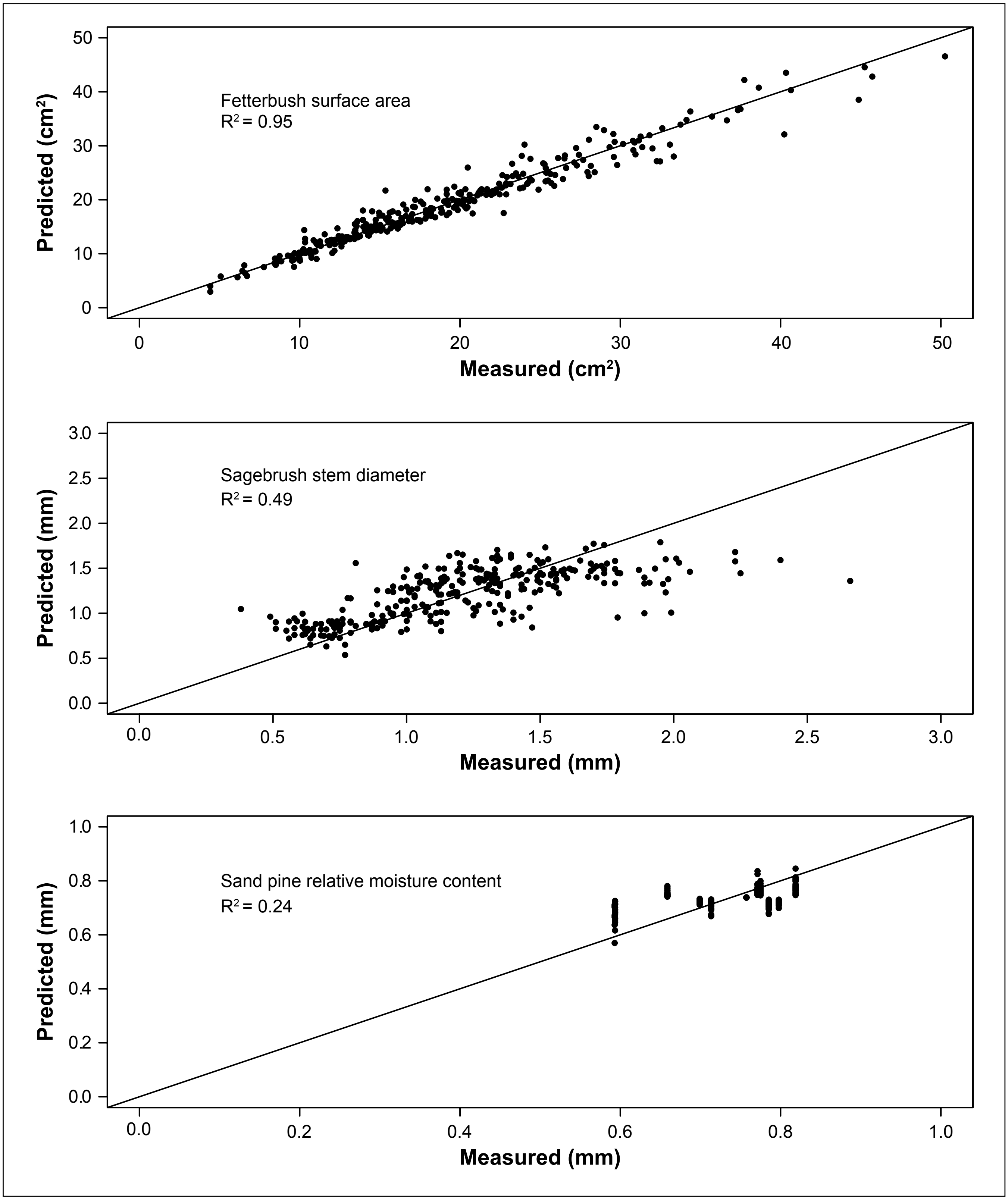

Figure 9—Representative plots for prediction models showing fetterbush surface area (top, $R^2 = 0.95$), sagebrush diameter (middle, $R^2 = 0.49$), and sand pine relative moisture content (bottom, $R^2 = 0.24$).

Conclusions

Physical properties and dimensions for 10 live fuels in the United States were measured throughout a 1-year period to determine if the properties and flammability changed over the year. Broadleaf samples consisted of whole leaves; needle samples consisted of a small length of branch with the foliage attached. Although sagebrush foliage comprises leaves rather than needles, the sagebrush samples were characterized as needle samples because the leaves are so small. Measurements included MC, RMC, apparent density, length, width, needle length, stem diameter, leaf thickness, leaf surface area, fresh mass, volatiles content, fixed-carbon content, ash content, and lipid content. We developed and used an alternate method for measuring foliage apparent density that used oil instead of water. Whole-leaf surface area measurements not requiring an assumed idealized shape were reported. The two-parameter Weibull distribution modeled foliage dry mass distributions to allow a user to calculate the dry mass for a single leaf or branch tip. Prediction equations based on sample dry mass and MC were developed for each measured property. Most measured sample characteristics did not change throughout the year, making the use of a seasonal parameter unnecessary. Sample characteristics that did change throughout the year were associated with changes in the other characteristics (usually MC) so that the models developed here are accurate for the entire year. It is anticipated that these models can be used in conjunction with bulk fuel description models and fuel placement models such as L-systems to describe the fuel matrix in detail for comprehensive fire spread models.

English Equivalents

When you know:	Multiply by:	To find:
Centimeters (cm)	0.394	Inches
Millimeters (mm)	0.0394	Inches
Square centimeters (cm^2)	0.155	Square inches
Cubic centimeters (cm^3)	0.061	Cubic inches
Cubic meters (m^3)	35.3	Cubic feet
Grams (g)	0.0352	Ounces
Kilograms (kg)	2.205	Pounds
Grams per cubic cm (g/cm^3)	0.0000624	Pounds per cubic foot

Literature Cited

Albini, F.A. 1976. Estimating wildfire behavior and effects. Gen. Tech. Rep. INT-GTR-30. Ogden, UT: U.S. Department of Agriculture, Forest Service, Intermountain Forest and Range Experiment Station. 92 p. http://www.fs.fed.us/rm/pubs_int/int_gtr030.pdf. (20 December 2016).

Bailey, R.L.; Dell, T.R. 1973. Quantifying diameter distributions with the Weibull function. Forest Science. 19: 97–104.

Barbier, N.; Couteron, P.; Gastelly-Etchegorry, J.P.; Proisy, C. 2012. Linking canopy images to forest structural parameters: potential of a modeling framework. Annals of Forest Science. 69: 305–311.

Bartelink, H.H. 1998. A model of dry matter partitioning in trees. Tree Physiology. 18: 91–101.

Behm, A.L.; Duryea, M.L.; Long, A.J.; Zipperer, W.C. 2004. Flammability of native understory species in pine flatwood and hardwood hammock ecosystems and implications for the wildland-urban interface. International Journal of Wildland Fire. 13: 355–365.

Britton, N.L.; Brown, A. 1913. An illustrated flora of the northern United States, Canada and the British Possessions. New York: Charles Scribner's Sons. 3 vols.

Brown, J.K. 1976. Estimating shrub biomass from basal stem diameters. Canadian Journal of Forest Research. 6: 153–158.

Brown, J.K. 1978. Weight and density of crowns of Rocky Mountain conifers. Res. Pap. INT-197. Ogden, UT: U.S. Department of Agriculture, Forest Service, Intermountain Forest and Range Experiment Station. 56 p. http://www.fs.fed.us/rm/pubs_int/int_rp197.pdf. (26 September 2016).

Bunsenberg, G. 2004. Wildfire management in the United States: the evolution of a policy failure. Review of Policy Research. 21: 145–156.

Burgan, R.E.; Susott, R.A. 1991. Influence of sample processing techniques and seasonal variation on quantities of volatile compounds of gallberry, saw-palmetto and wax myrtle. International Journal of Wildland Fire. 1: 57–62.

Burnham, K.P.; Anderson, D.R. 2004. Multimodel inference: understanding AIC and BIC in model selection. Sociological Methods & Research. 33: 261–304.

Clark, M.M.; Fletcher, T.H.; Linn, R.R. 2010. A sub-grid, mixture-fraction-based thermodynamic equilibrium model for gas phase combustion in FIRETEC: development and results. International Journal of Wildland Fire. 19: 202–212.

Coen, J.L.; Cameron, M.; Michalakes, J.; Patton, E.G.; Riggan, P.J.; Yedinak, K.M. 2013. WRF-Fire: coupled weather-wildland fire modeling with the Weather Research and Forecasting Model. Journal of Applied Meteorology and Climatology. 52: 16–38.

Coen, J.L.; Riggan, P.J. 2014. Simulation and thermal imaging of the 2006 Esperanza Wildfire in southern California: application of a coupled weather-wildland fire model. International Journal of Wildland Fire. 23: 755–770.

Cohen, J.D. 1986. Estimating fire behavior with FIRECAST: user's manual. Gen. Tech. Rep. PSW-90. Berkeley, CA: U.S. Department of Agriculture, Forest Service, Pacific Southwest Forest and Range Experiment Station. 11 p. http://www.fs.fed.us/psw/publications/documents/psw_gtr090/psw_gtr090.pdf. (26 September 2016).

Cohen, J.; Bradshaw, B. 1986. Fire behavior modeling-a decision tool. In: Koonce, A.L., ed. Proceedings: prescribed burning in the Midwest: state of the art symposium. 162 p. http://www.fs.fed.us/psw/publications/cohen/psw_1986_cohen001.pdf. (20 December 2016).

Conrad, C.E. 1987. Common shrubs of chaparral and associated ecosystems of southern California. Gen. Tech. Rep. PSW-99. Berkeley, CA: U.S. Department of Agriculture, Forest Service, Pacific Southwest Forest and Range Experiment Station. 86 p. http://www.fs.fed.us/psw/publications/documents/psw_gtr099/psw_gtr099.pdf. (26 September 2016).

Countryman, C.M. 1982. Physical characteristics of some northern California brush fuels. Gen. Tech. Rep. PSW-61. Berkeley, CA: U.S. Department of Agriculture, Forest Service, Pacific Southwest Forest and Range Experiment Station. 8 p. http://www.fs.fed.us/psw/publications/documents/psw_gtr061/psw_gtr061.pdf. (26 September 2016).

Countryman, C.M.; Philpot, C.W. 1970. Physical characteristics of chamise as a wildland fuel. Res. Pap. PSW-66. Berkeley, CA: U.S. Department of Agriculture, Forest Service, Pacific Southwest Forest and Range Experiment Station. 16 p. http://www.fs.fed.us/psw/publications/documents/psw_rp066/psw_rp066.pdf. (26 September 2016).

Cruz, M.G.; Alexander, M.E.; Wakimoto, R.H. 2003. Assessing canopy fuel stratum characteristics in crown fire prone fuel types of western North America. International Journal of Wildland Fire. 12: 39–50.

Delignette-Muller, M.L.; Dutang, C. 2015. fitdistrplus: an R package for fitting distributions. Journal of Statistical Software. 64(4): doi:10.18637/jss.v064.i04.

Engstrom, J.D.; Butler, J.K.; Smith, S.G.; Baxter, L.L.; Fletcher, T.H.; Weise, D.R. 2004. Ignition behavior of live California chaparral leaves. Combustion Science and Technology. 176: 1577–1591.

Ezekiel, M. 1930. The sampling variability of linear and curvilinear regressions: a first approximation to the reliability of the results secured by the graphic "Successive Approximation" method. The Annals of Mathematical Statistics. 1: 275–315.

Fahnestock, G.R.; Key, W.K. 1971. Weight of brushy forest fire fuels from photographs. Forest Science. 17(1): 119–124.

Fernandes, P.M.; Rego, F.C. 1998. A new method to estimate fuel surface area-to-volume ratio using water immersion. International Journal of Wildland Fire. 8: 59–66.

Finney, M.A. 1998. FARSITE: Fire Area Simulator—model development and evaluation. Res. Pap. RMRS-RP-4. Fort Collins, CO: U.S. Department of Agriculture, Forest Service, Rocky Mountain Research Station. 47 p. http://www.fs.fed.us/rm/pubs/rmrs_rp004.pdf. (26 September 2016).

Fire Executive Council. 2009. Guidance for implementation of federal wildland fire management policy. Washington, DC: U.S. Department of Agriculture and U.S. Department of the Interior. 20 p. https://www.nifc.gov/policies/policies_documents/GIFWFMP.pdf. (26 September 2016).

Fishman, G.S. 1997. Monte Carlo: concepts, algorithms, and applications. New York: Springer Series in Operations Research and Financial Engineering. 698 p.

Fleming, R.A. 2001. The Weibull model and an ecological application: describing the dynamics of foliage biomass on Scots pine. Ecological Modelling. 138: 309–319.

Fletcher, T.H.; Pickett, B.M.; Smith, S.G.; Spittle, G.S.; Woodhouse, M.M.; Haake, E.; Weise, D.R. 2007. Effects of moisture on ignition behavior of moist California chaparral and Utah leaves. Combustion Science and Technology. 179: 1183–1203.

Fons, W.L. 1946. Analysis of fire spread in light forest fuels. Journal of Agricultural Research. 72: 93–121.

Frandsen, W.H. 1983. Modeling big sagebrush as a fuel. Journal of Range Management. 36(5): 596–600.

Gallacher, J.R. 2016. The influence of season, heating mode and slope angle on wildland fire behavior. Provo, UT: Brigham Young University. 238 p. Ph.D. dissertation.

Gallacher, J.R.; Lansinger, V.; Hansen, S.; Ellsworth, T.; Weise, D.R.; Fletcher, T.H. 2016. Physical and chemical properties of the foliage of 10 live wildland fuels. Fort Collins, CO: U.S. Department of Agriculture, Forest Service, Forest Service Research Data Archive. http://dx.doi.org/10.2737/RDS-2016-0023. (26 September 2016).

Gujarati, D.N. 2003. Basic econometrics. 4th ed. New York: McGraw-Hill. 1003 p.

Heinsch, F.A.; Andrews, P.L. 2010. BehavePlus Fire Modeling System, Version 5.0: design and features. Gen. Tech. Rep. RMRS-GTR-249. Fort Collins, CO: U.S. Department of Agriculture, Forest Service, Rocky Mountain Research Station. 111 p. http://www.fs.fed.us/rm/pubs/rmrs_gtr249.pdf. (26 September 2016).

Helgerson, O.T.; Cromack, K.; Stafford, S.; Miller, R.E.; Slagle, R. 1988. Equations for estimating above-ground components of young Douglas-fir and red alder in a coastal Oregon plantation. Canadian Journal of Forest Research. 18: 1082–1085.

Hough, W.A. 1969. Caloric values of some forest fuels of the southern United States. Res. Note SE-120. Asheville, NC: U.S. Department of Agriculture, Forest Service, Southeastern Forest Experiment Station. 6 p. http://www.srs.fs.usda.gov/pubs/rn/rn_se120.pdf. (26 September 2016).

Hough, W.A.; Albini, F.A. 1978. Predicting fire behavior in palmetto-gallberry fuel complexes. Res. Pap. SE-174. Asheville, NC: U.S. Department of Agriculture, Forest Service, Southeastern Forest Experiment Station. 44 p. http://www.srs.fs.fed.us/pubs/rp/rp_se174.pdf. (26 September 2016).

Hull, M.K.; O'Dell, C.A.; Schroeder, M.J. 1966. Critical fire weather patterns-their frequency and levels of fire danger. Berkeley, CA: U.S. Department of Agriculture, Forest Service, Pacific Southwest Forest and Range Experiment Station. 40 p.

Jolly, W.M.; Hadlow, A.M.; Huguet, K. 2014. De-coupling seasonal changes in water content and dry matter to predict live conifer foliar moisture content. International Journal of Wildland Fire. 23: 480–489.

Keane, R.E.; Gray, K.; Bacciu, V. 2012. Spatial variability of wildand fuel characteristics in northern Rocky Mountain ecosystems. Res. Pap. RMRS-RP-98. Fort Collins, CO: U.S. Department of Agriculture, Forest Service, Rocky Mountain Research Station. 56 p. http://www.fs.fed.us/rm/pubs/rmrs_rp098.pdf. (26 September 2016).

Keyser, T.; Smith, F.W. 2010. Influence of crown biomass estimators and distribution on canopy fuel characteristics in ponderosa pine stands of the Black Hills. Forest Science. 56: 156–165.

Linn, R.; Winterkamp, J.; Colman, J.J.; Edminster, C.; Bailey, J.D. 2005. Modeling interactions between fire and atmosphere in discrete element fuel beds. International Journal of Wildland Fire. 14: 37–48.

Linn, R.R. 1997. A transport model for prediction of wildfire behavior. Las Cruces, NM: New Mexico State University. 195 p. Ph.D. dissertation.

Linn, R.R.; Cunningham, P. 2005. Numerical simulations of grass fires using a coupled atmosphere-fire model: basic fire behavior and dependence on wind speed. Journal of Geophysical Research-Atmospheres. 110: D13107. doi: 10.1029/2004JD005597.

Loudermilk, E.L.; Hiers, J.K.; O'Brien, J.J.; Mitchell, R.J.; Singhania, A.; Fernandez, J.C.; Cropper, W.P.; Slatton, K.C. 2009. Ground-based LIDAR: a novel approach to quantify fine-scale fuelbed characteristics. International Journal of Wildland Fire. 18: 676–685.

Ludwig, J.A.; Reynolds, J.F.; Whitson, P.D. 1975. Size-biomass relationships of several Chihuahuan Desert shrubs. American Midland Naturalist. 94: 451–461.

Lyons, P.R.A.; Weber, R.O. 1993. Geometrical effects on flame spread rate for wildland fine fuels. Combustion Science and Technology. 89: 153–165.

Maguire, D.A.; Bennett, W.S. 1996. Patterns in vertical distribution of foliage in young coastal Douglas-fir. Canadian Journal of Forest Research. 26: 1991–2005.

Marino, E.; Dupuy, J.L.; Pimont, F.; Guijarro, M.; Hernando, C.; Linn, R. 2012. Fuel bulk density and fuel moisture content effects on fire rate of spread: a comparison between FIRETEC model predictions and experimental results in shrub fuels. Journal of Fire Sciences. 30: 277–299.

Mason, R.L.; Gunst, R.F.; Hess, J.L. 1989. Statistical design and analysis of experiments: with applications to engineering and science. New York: Wiley. 692 p.

McAllister, S.; Weise, D.R. 2017. Effects of season on ignition of live wildland fuels using the FIST apparatus. Combustion Science and Technology. doi: 10.1080/00102202.2016.1206086.

McGrattan, K.B.; Forney, G.P. 2004. Fire dynamics simulator (Version 4)—user's guide. NIST Spec. Publ. 1019. Gaithersburg, MD: U.S. Department of Commerce, National Institute of Standards and Technology, Technology Administration. 98 p. http://fire.nist.gov/bfrlpubs/fire04/PDF/f04099.pdf. (26 September 2016).

McNab, W.H.; Edwards, M.B., Jr.; Hough, W.A. 1978. Estimating fuel weights in slash pine-palmetto stands. Forest Science. 24: 345–358.

Mell, W.; Jenkins, M.A.; Gould, J.; Cheney, P. 2007. A physics-based approach to modelling grassland fires. International Journal of Wildland Fire. 16: 1–22.

Mell, W.; Maranghides, A.; McDermott, R.; Manzello, S.L. 2009. Numerical simulation and experiments of burning Douglas-fir trees. Combustion and Flame. 156(10): 2023–2041.

Narender, K.; Rao, A.S.M.; Rao, K.G.K.; Krishna, N.G. 2013. Thermo physical properties of wrought aluminum alloys 6061, 2219 and 2014 by gamma ray attenuation method. Thermochimica Acta. 569: 90–96.

Papió, C.; Trabaud, L. 1990. Structural characteristics of fuel components of five mediterranean shrubs. Forest Ecology and Management. 35: 249–259.

Parsons, R.A.; Mell, W.E.; McCauley, P. 2011. Linking 3D spatial models of fuels and fire: effects of spatial heterogeneity on fire behavior. Ecological Modelling. 222: 679−691.

Pereira, J.M.C.; Sequeira, N.M.S.; Carreiras, J.M.B. 1995. Structural properties and dimensional relations of some Mediterranean shrub fuels. International Journal of Wildland Fire. 5: 35−42.

Peterson, S.H.; Morais, M.E.; Carlson, J.M.; Dennison, P.E.; Roberts, D.A.; Moritz, M.A.; Weise, D.R. 2009. Using HFire for spatial modeling of fire spread in shrublands. Res. Pap. PSW-RP-259. Albany, CA: U.S. Department of Agriculture, Forest Service, Pacific Southwest Research Station. 44 p. http://www.fs.fed.us/psw/publications/documents/psw_rp259/psw_rp259.pdf. (26 September 2016).

Philpot, C.W. 1969. Seasonal changes in heat content and ether extractive content of chamise. Res. Pap. INT-61. Ogden, UT: U.S. Department of Agriculture, Forest Service, Intermountain Forest and Range Experiment Station. 10 p. https://ia601005.us.archive.org/16/items/seasonalchangesi61phil/seasonalchangesi61phil.pdf. (26 September 2016).

Pickett, B.M. 2008. Effects of moisture on combustion of live wildland forest fuels. Provo, UT: Brigham Young University. 208 p. Ph.D. dissertation.

Pinheiro, J.C.; Bates, D.M. 2000. Mixed-effects models in S and S-PLUS. New York: Springer Statistics and Computing. 528 p.

Powell, D.C. 2013. Field guide to forest plants of south-central Colorado. R2-ECOL-87–1. Lakewood, CO: U.S. Department of Agriculture, Forest Service, Rocky Mountain Region. 296 p. http://www.fs.usda.gov/Internet/FSE_DOCUMENTS/stelprd3798303.pdf. (26 September 2016).

Prince, D.R. 2014. Measurement and modeling of fire behavior in leaves and sparse shrubs. Provo, UT: Brigham Young University. 307 p. Ph.D. dissertation.

Prince, D.R.; Fletcher, M.E.; Shen, C.; Fletcher, T.H. 2014. Application of L-systems to geometrical construction of chamise and juniper shrubs. Ecological Modelling. 273: 86–95.

R Core Team. 2013. R: a language and environment for statistical computing. Vienna, Austria: R Foundation for Statistical Computing. http://www.R-project.org/. (26 September 2016).

Reinhardt, E.; Scott, J.; Gray, K.; Keane, R. 2006. Estimating canopy fuel characteristics in five conifer stands in the western United States using tree and stand measurements. Canadian Journal of Forest Research. 36: 2803–2814.

Riccardi, C.L.; Prichard, S.J.; Sandberg, D.V.; Ottmar, R.D. 2007. Quantifying physical characteristics of wildland fuels using the fuel characteristic classification system. Canadian Journal of Forest Research. 37: 2413–2420.

Rinne, H. 2008. The Weibull distribution: a handbook. Boca Raton, FL: CRC Press. 808 p.

Rothermel, R.C. 1972. A mathematical model for predicting fire spread in wildland fuels. Res. Pap. INT-115. Ogden, UT: U.S. Department of Agriculture, Forest Service, Intermountain Forest and Range Experiment Station. 40 p. http://www.fs.fed.us/rm/pubs_int/int_rp115.pdf. (26 September 2016).

Ryan, K.C.; Pickford, S.G. 1978. Physical properties of woody fuels in the Blue Mountains of Oregon and Washington. Res. Note PNW-315. Portland, OR: U.S. Department of Agriculture, Forest Service, Pacific Northwest Forest and Range Experiment Station. 14 p.

Sackett, S.S. 1980. Woody fuel particle size and specific gravity of southwestern tree species. Res. Note RM-389. Fort Collins, CO: U.S. Department of Agriculture, Forest Service, Rocky Mountain Forest and Range Experiment Station. 4 p.

Schlecht, R.M.; Affleck, D.L.R. 2014. Branch aggregation and crown allometry condition the precision of randomized branch sampling estimators of conifer crown mass. Canadian Journal of Forest Research. 44: 499–508.

Schreuder, H.T.; Swank, W.T. 1974. Coniferous stands characterized with the Weibull distribution. Canadian Journal of Forest Research. 4: 518–523.

Schwilk, D.W. 2003. Flammability is a niche construction trait: canopy architecture affects fire intensity. American Naturalist. 162: 725–733.

Seielstad, C.; Stonesifer, C.; Rowell, E.; Queen, L. 2011. Deriving fuel mass by size class in Douglas-fir (*Pseudotsuga menziesii*) using terrestrial laser scanning. Remote Sensing. 3: 1691–1709.

Shen, C. 2013. Application of fuel element combustion properties to a semi-empirical flame propagation model for live wildland Utah shrubs. Ogden, UT: Brigham Young University. 98 p. M.S. thesis.

Shen, C.; Fletcher, T.H. 2015. Fuel element combustion properties for live wildland Utah shrubs. Combustion Science and Technology. 187: 428–444.

Skowronski, N.; Clark, K.; Nelson, R.; Hom, J.; Patterson, M. 2007. Remotely sensed measurements of forest structure and fuel loads in the pinelands of New Jersey. Remote Sensing of Environment. 108: 123–129.

Skowronski, N.S.; Clark, K.L.; Duveneck, M.; Hom, J. 2011. Three-dimensional canopy fuel loading predicted using upward and downward sensing LiDAR systems. Remote Sensing of Environment. 115: 703-714.

Smith, D.M. 1954. Maximum moisture content method for determining specific gravity of small wood samples. Report 2014. Madison, WI: U.S. Department of Agriculture, Forest Service, Forest Products Laboratory. 8 p. http://ir.library.oregonstate.edu/xmlui/bitstream/handle/1957/2445. (26 September 2016).

Stephens, S.L.; Ruth, L.W. 2005. Federal forest-fire policy in the United States. Ecological Applications. 15: 532–542.

Sullivan, A.L. 2009a. Wildland surface fire spread modelling, 1990–2007: 1-physical and quasi-physical models. International Journal of Wildland Fire. 18: 349–368.

Sullivan, A.L. 2009b. Wildland surface fire spread modelling, 1990–2007: 2-empirical and quasi-empirical models. International Journal of Wildland Fire. 18: 369–386.

Sullivan, A.L. 2009c. Wildland surface fire spread modelling, 1990–2007: 3-simulation and mathematical analogue models. International Journal of Wildland Fire. 18: 387–403.

U.S. Department of Agriculture, Forest Service [USDA FS]. 2012. FCCS inferred variables. Seattle, WA: U.S. Department of Agriculture, Forest Service, Pacific Northwest Research Station. http://www.fs.fed.us/pnw/fera/fccs/inferred_variables/. (26 September 2016).

U.S. Department of Agriculture, Natural Resources Conservation Service. [USDA NRCS] 2016. PLANTS database. http://plants.usda.gov/java/. (28 September 2016).

van Wagtendonk, J.W.; Benedict, J.M.; Sydoriak, W.M. 1996. Physical properties of woody fuel particles of Sierra Nevada conifers. International Journal of Wildland Fire. 6: 117–123.

Weatherley, P.E. 1950. Studies in the water relations of the cotton plant. I: The field measurement of water deficits in leaves. New Phytologist. 49(1): 81–97.

Weber, R.O. 1991. Modelling fire spread through fuel beds. Progress in Energy and Combustion Science. 17: 67–82.

Weise, D.R.; Koo, E.; Zhou, X.; Mahalingam, S.; Morandini, F.; Balbi, J.-H. 2016. Fire spread in chaparral—a comparison of laboratory data and model predictions in burning live fuels. International Journal of Wildland Fire. 25: 980–994.

Weise, D.R.; Mahalingam, S.; Fletcher, T.H.; Shotorban, B.; McAllister, S.S.; Jolly, W.M. 2015. Determination of the effects of heating mechanisms and moisture content on ignition of live fuels. Project 11-1-4-19; final report. Boise, ID: Joint Fire Science Program. 26 p. http://www.firescience.gov/projects/11-1-4-19/project/11-1-4-19_final_report.pdf. (26 September 2016).

Weise, D.R.; White, R.H.; Beall, F.C.; Etlinger, M. 2005. Use of the cone calorimeter to detect seasonal differences in selected combustion characteristics of ornamental vegetation. International Journal of Wildland Fire. 14: 321–338.

Weise, D.R.; Wright, C.S. 2014. Wildland fire emissions, carbon and climate: characterizing wildland fuels. Forest Ecology and Management. 317: 26–40.

Werth, P. 2015a. Critical fire weather patterns—Eastern United States, Canada, and Australia [webinar]. Wildland Fire Lessons Learned Center, International Association of Wildland Fire, Joint Fire Science Program. 78. https://www.youtube.com/watch?v=qWFTFvpYX68&feature=youtu.be. (26 September 2016).

Werth, P. 2015b. Critical fire weather patterns—Western United States. [webinar]. Wildland Fire Lessons Learned Center Wildland Fire Lessons Learned Center, International Association of Wildland Fire, Joint Fire Science Program. 69 min. https://www.youtube.com/watch?v=pTjrKcKCnDQ&feature=youtu.be. (26 September 2016).

White, R.H.; Zipperer, W.C. 2010. Testing and classification of individual plants for fire behaviour: plant selection for the wildland-urban interface. International Journal of Wildland Fire. 19: 213–227.

Williams, R.A. 1989. Use of randomized branch and importance sampling to estimate loblolly pine biomass. Southern Journal of Applied Forestry. 13: 181–184.

Wright, C.S. 2013. Fuel consumption models for pine flatwoods fuel types in the Southeastern United States. Southern Journal of Applied Forestry. 37: 148–159.

Yashwanth, B.L.; Shotorban, B.; Mahalingam, S.; Lautenberger, C.W.; Weise, D.R. 2016. A numerical investigation of the influence of radiation and moisture content on pyrolysis and ignition of a leaf-like fuel element. Combustion and Flame. 163: 301–316.

Yashwanth, B.L.; Shotorban, B.; Mahalingam, S.; Weise, D.R. 2015. An investigation of the influence of heating modes on ignition and pyrolysis of woody wildland fuel. Combustion Science and Technology. 187: 780–796.

Appendix: Two-Parameter Weibull Distribution for Mass Data

The empirical and fitted probability density (PDF) functions, empirical and fitted cumulative distribution functions (CDF), empirical and fitted quantiles (Q-Q plot), and empirical and fitted probabilities (P-P plot) for each species are presented here. A summary of the fitted distribution including correlation of the scale (a) and shape (b) parameters as well as details of the goodness of fit statistics (Kolmogorov-Smirnov, Anderson-Darling, and Cramer-von Mises) are also presented. A 95^{th}-percentile confidence interval for the fitted CDF, represented by the grey band, was estimated using parametric bootstrapping with the *bootdist* function in the *fitdistrplus* package (Delignette-Muller and Dutang 2015).

The species plots are arranged in the order of appearance in the table above in figure 10. For each species, the upper left graph is of the fitted PDF and a histogram of the data. The lower left graph illustrates the empirical CDF and the 95 percent confidence interval for the fitted CDF. The upper right graph plots the empirical and fitted quantiles while the lower right graph shows the fitted and empirical probabilities.

Table 5—Parameter estimates ($\hat{a},\hat{b}$) and goodness of fit measures of the 2-parameter Weibull distribution for fuel particle oven-dry mass

Species	Scale		Shape		$\rho_{\hat{a},\hat{b}}$	AIC
	$\hat{a}$	$S_{\hat{a}}$	$\hat{b}$	$S_{\hat{b}}$		
Ceanothus	0.100	0.003	2.508	0.107	0.337	-1055
Gallberry	0.134	0.003	2.685	0.120	0.321	-984
Chamise	0.157	0.004	2.128	0.082	0.333	-890
Gambel oak	0.261	0.012	1.929	0.123	0.323	-215
Big sagebrush	0.258	0.009	1.796	0.076	0.330	-421
Fetterbush	0.316	0.008	2.474	0.105	0.331	-442
Manzanita	0.373	0.009	2.621	0.107	0.333	-379
Douglas-fir	0.677	0.018	2.447	0.108	0.330	18
Sand pine	0.753	0.016	2.890	0.131	0.313	21
Lodgepole pine	1.489	0.036	2.941	0.142	0.332	292
			Goodness of fit			
	Kolmogorov-Smirnov		Anderson-Darling		Cramér-von Mises	
Ceanothus	0.114	R	5.442	R	0.904	R
Gallberry	0.050	NR	0.933	R	0.158	R
chamise	0.077	R	3.954	R	0.552	R
Gambel oak	0.068	NR	0.834	R	0.119	NR
Big sagebrush	0.061	NR	2.192	R	0.245	NR
Fetterbush	0.088	R	3.388	R	0.539	R
Manzanita	0.073	NR	3.749	R	0.529	R
Douglas-fir	0.077	NR	2.590	R	0.428	R
Sand pine	0.041	NR	0.509	NR	0.066	NR
Lodgepole pine	0.068	NR	2.389	R	0.329	R

Note: $S_{\hat{a}}$, $S_{\hat{b}}$, $\rho_{\hat{a},\hat{b}}$ are the standard errors for the parameters estimates and the correlation of the estimates, respectively. AIC is the Akaike Information Criterion. For each measure of goodness of fit, the statistic and its significance are reported. R indicates rejection of the null hypothesis at $\alpha = 0.05$, NR indicates the null hypothesis was not rejected.

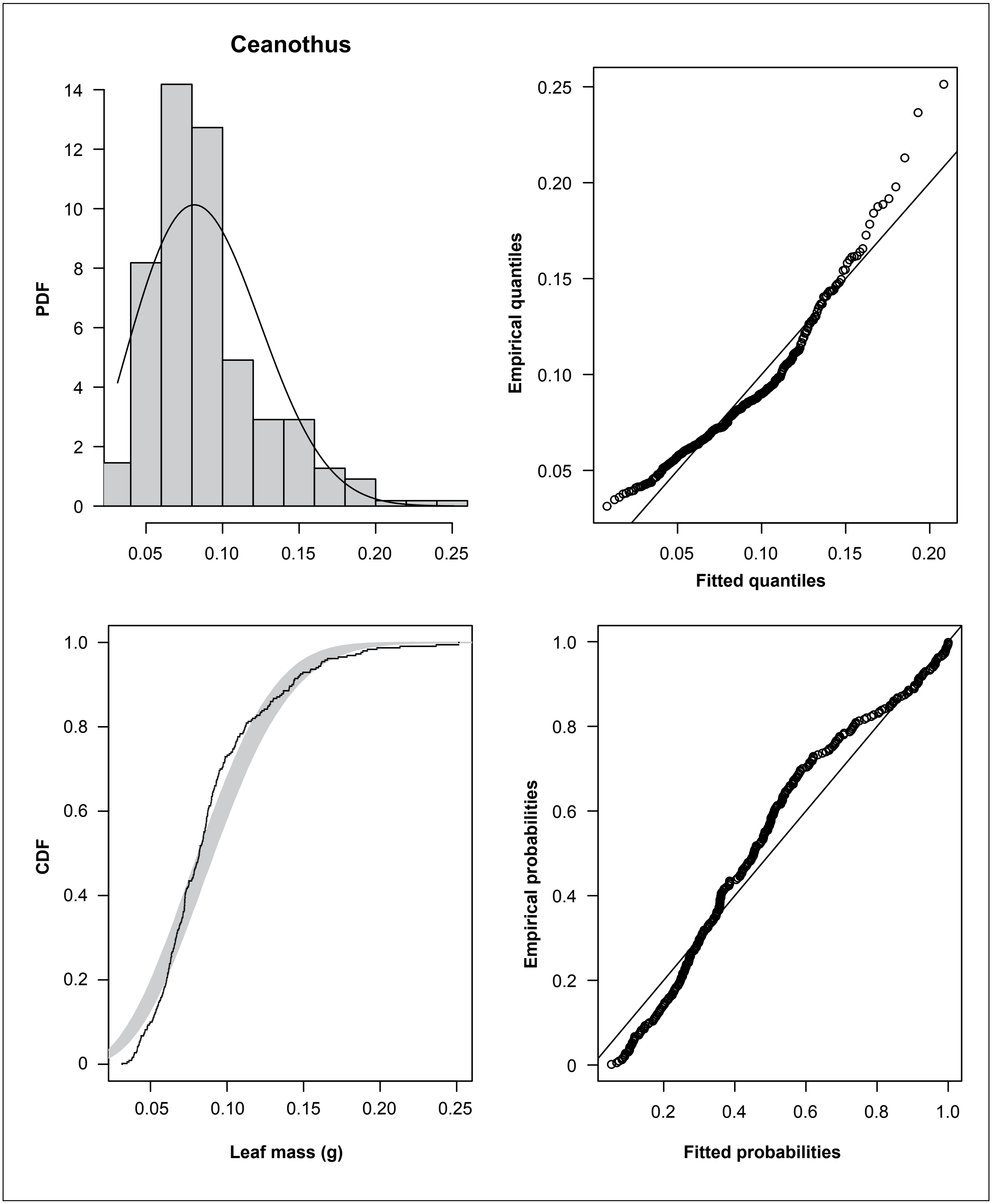

Figure 10—Graphical measures of goodness of fit of Weibull distribution for foliage mass for 10 live fuels in the United States. PDF = fitted probability density, CDF = cumulative distribution functions.

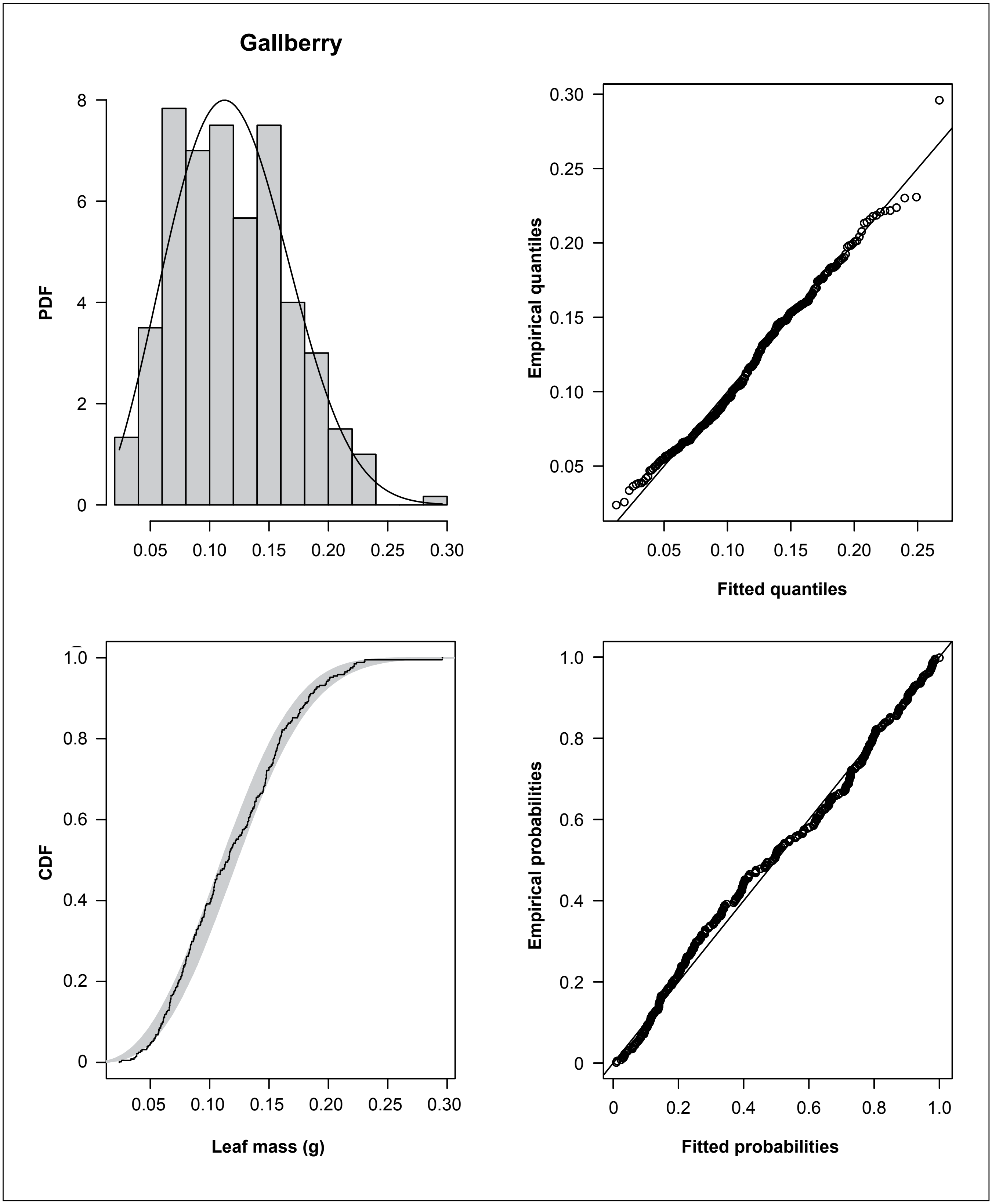

Figure 10—Continued.

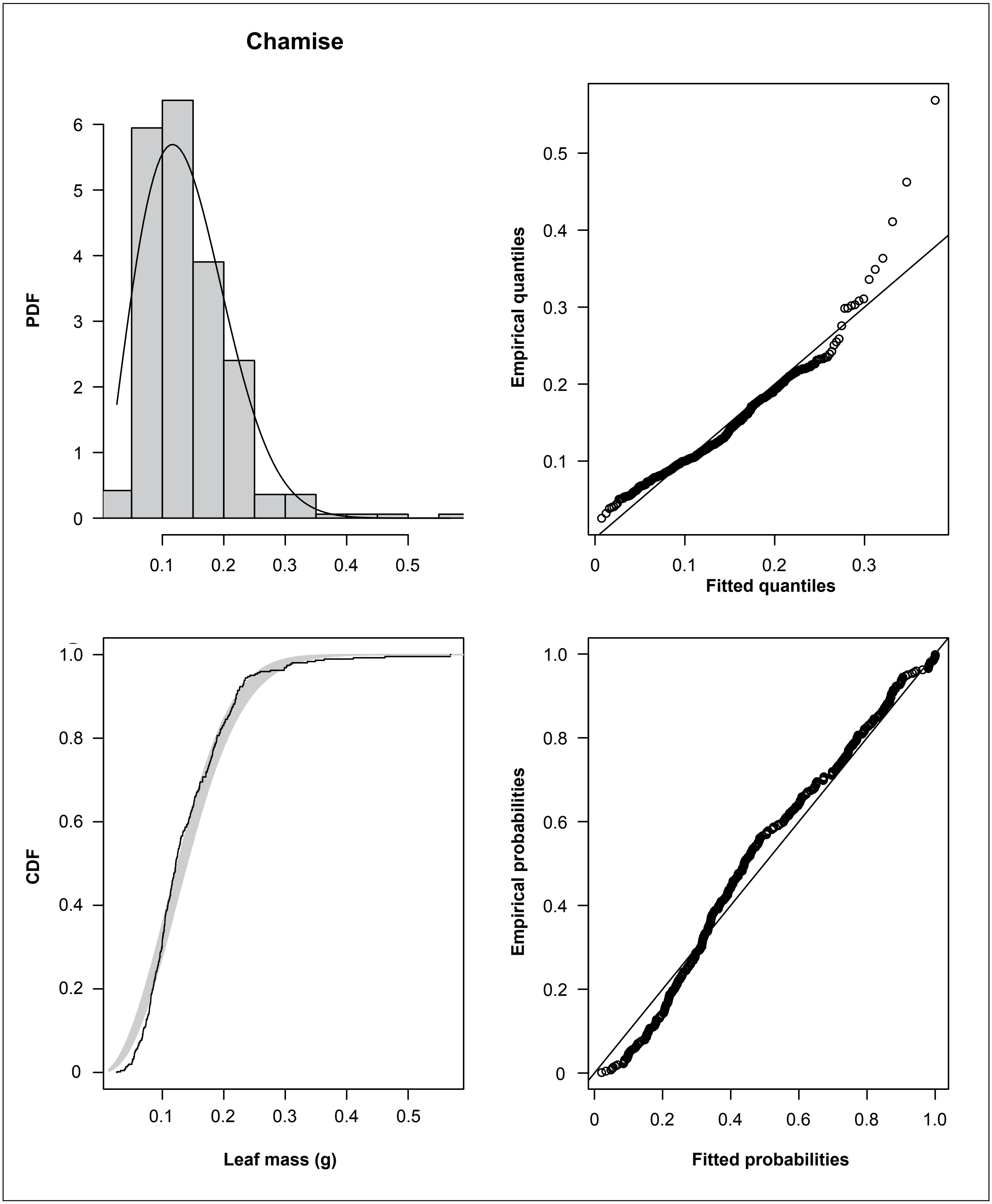

Figure 10—Continued.

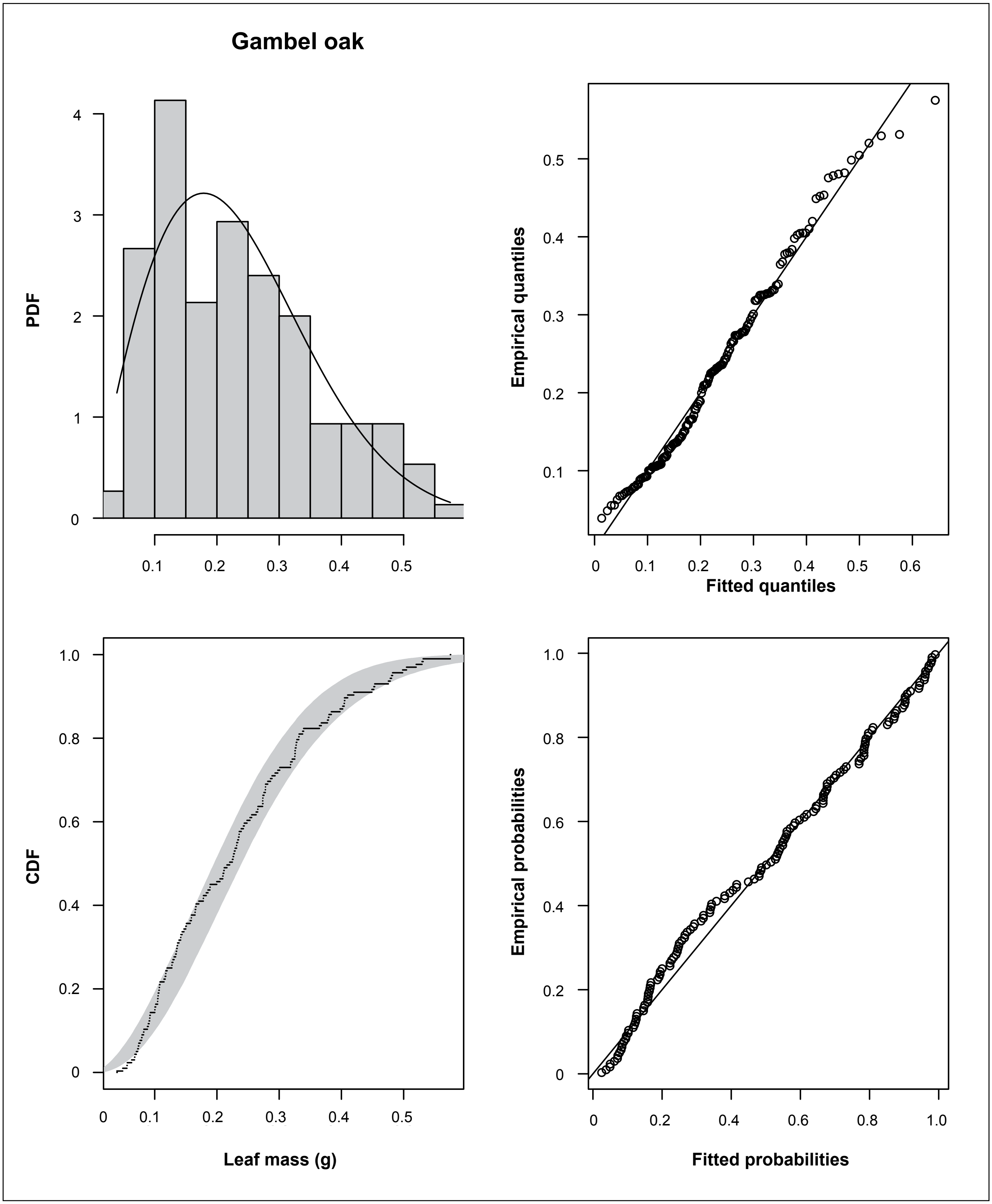

Figure 10—Continued.

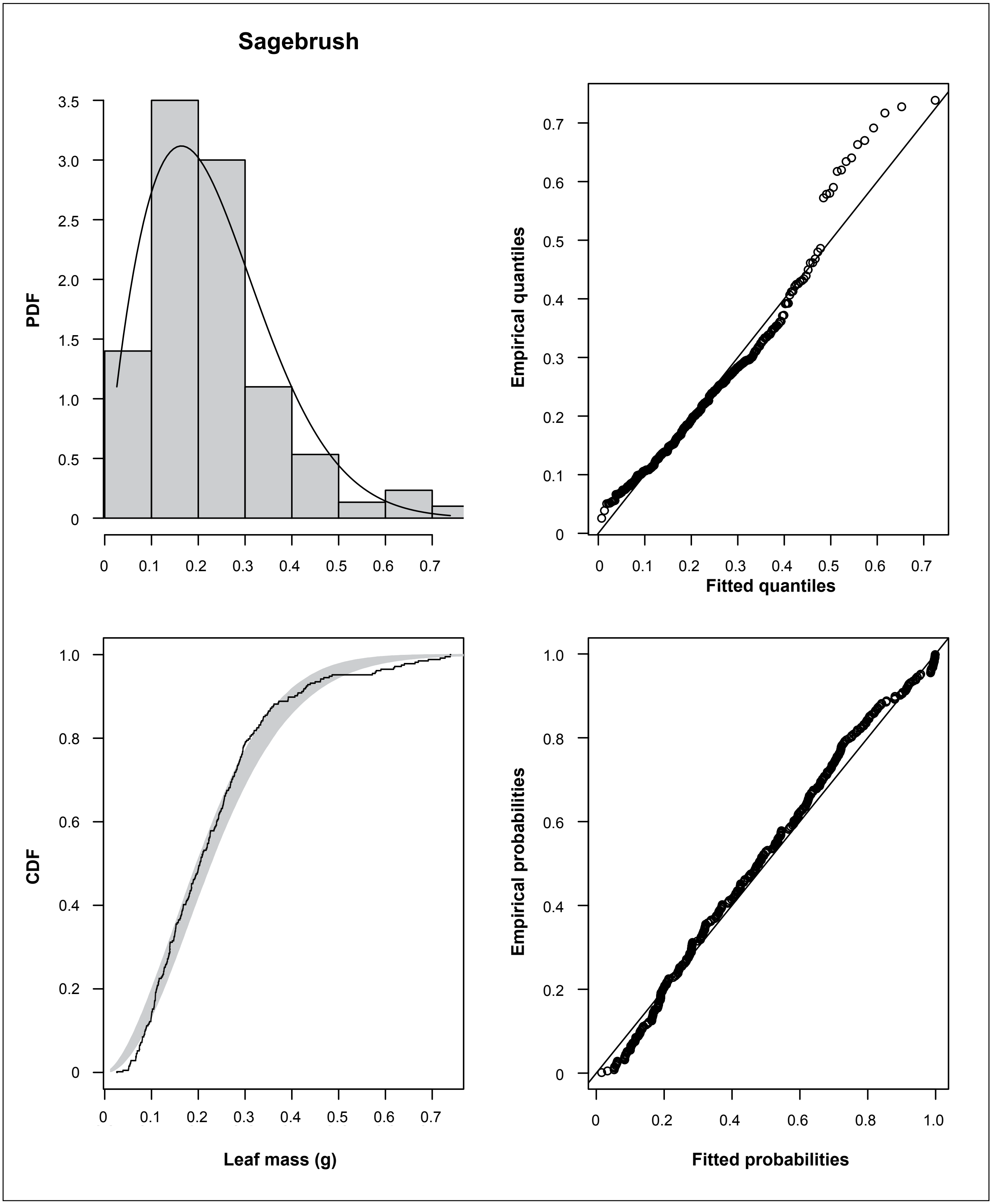

Figure 10—Continued.

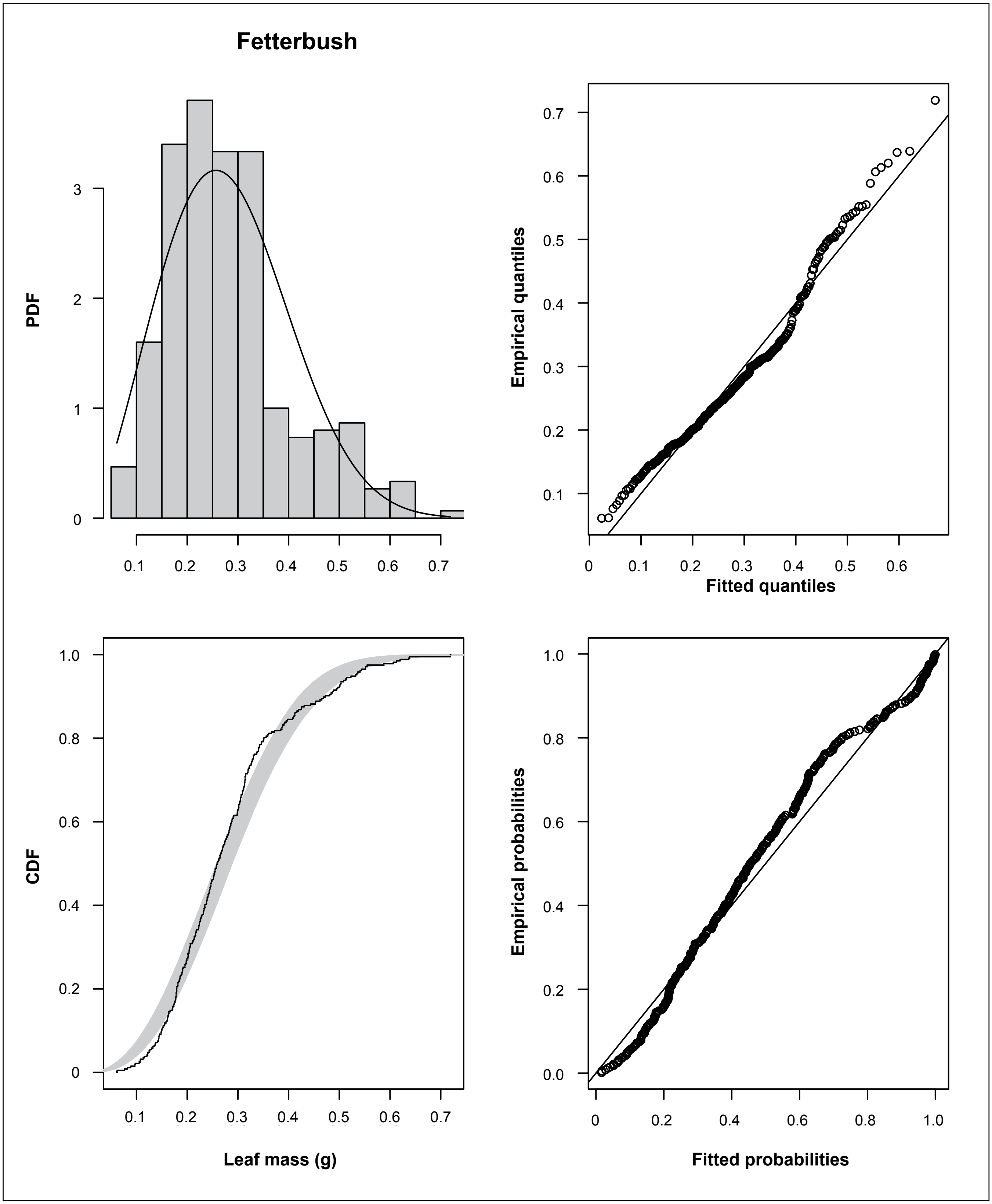

Figure 10—Continued.

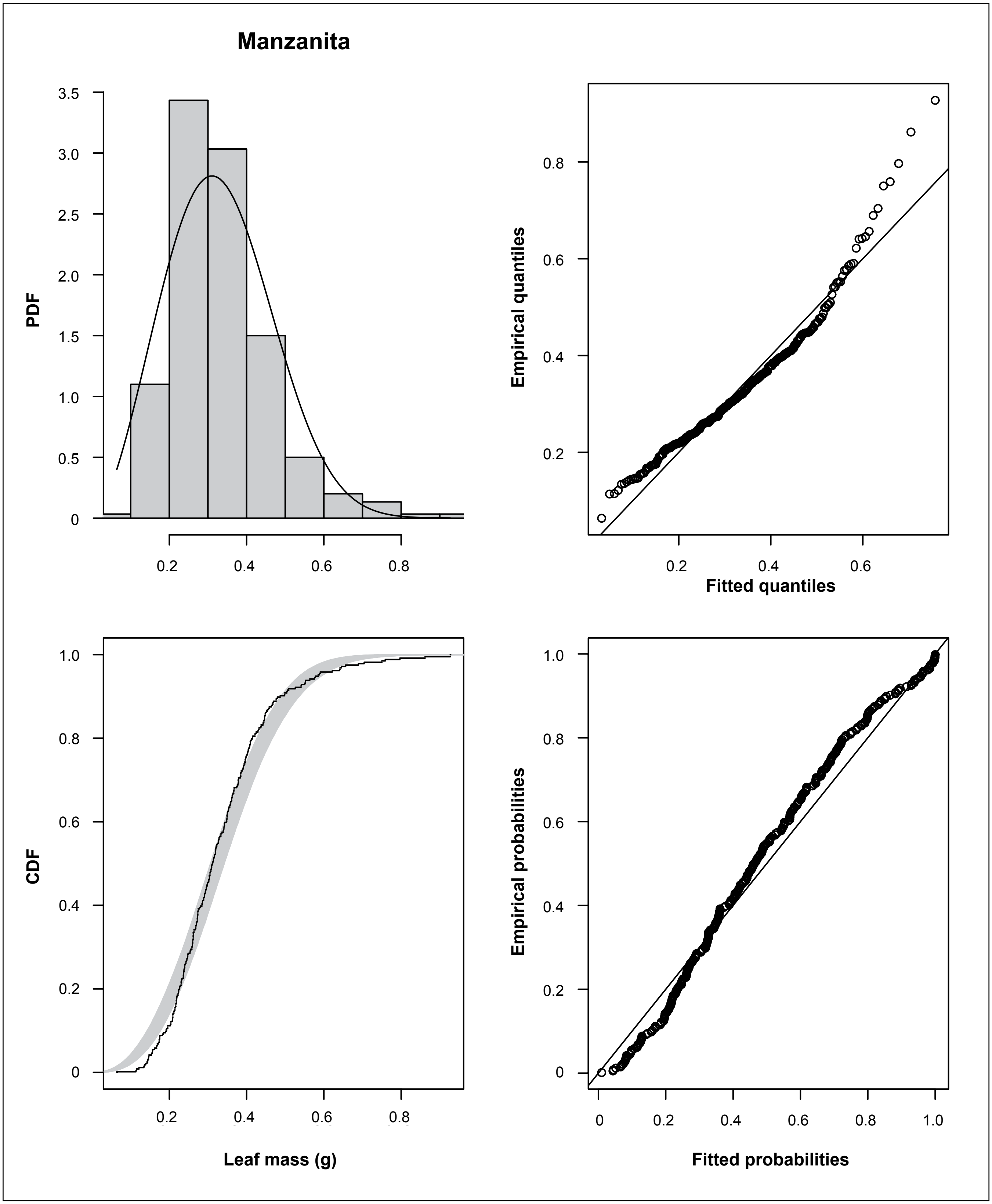

Figure 10—Continued.

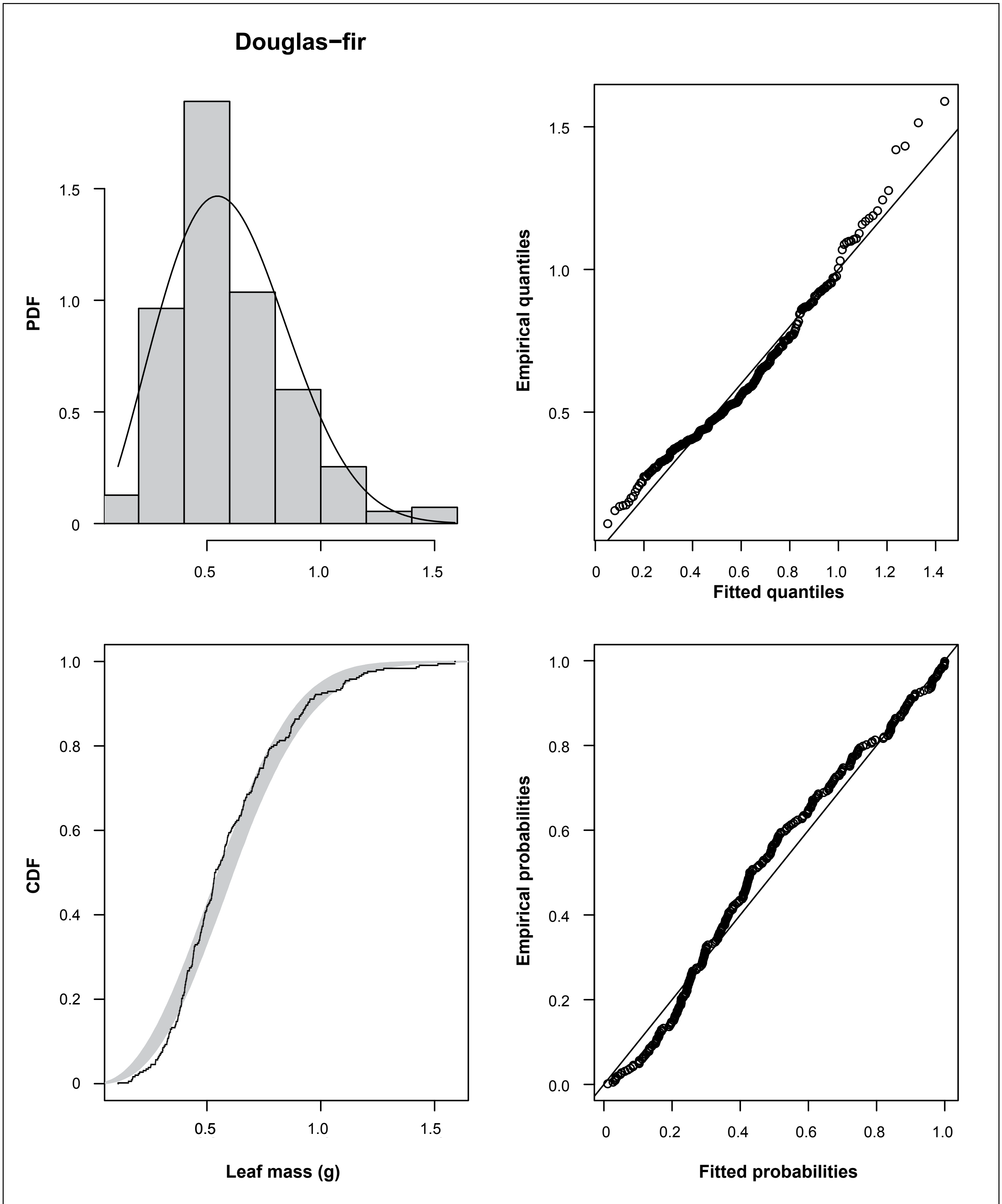

Figure 10—Continued.

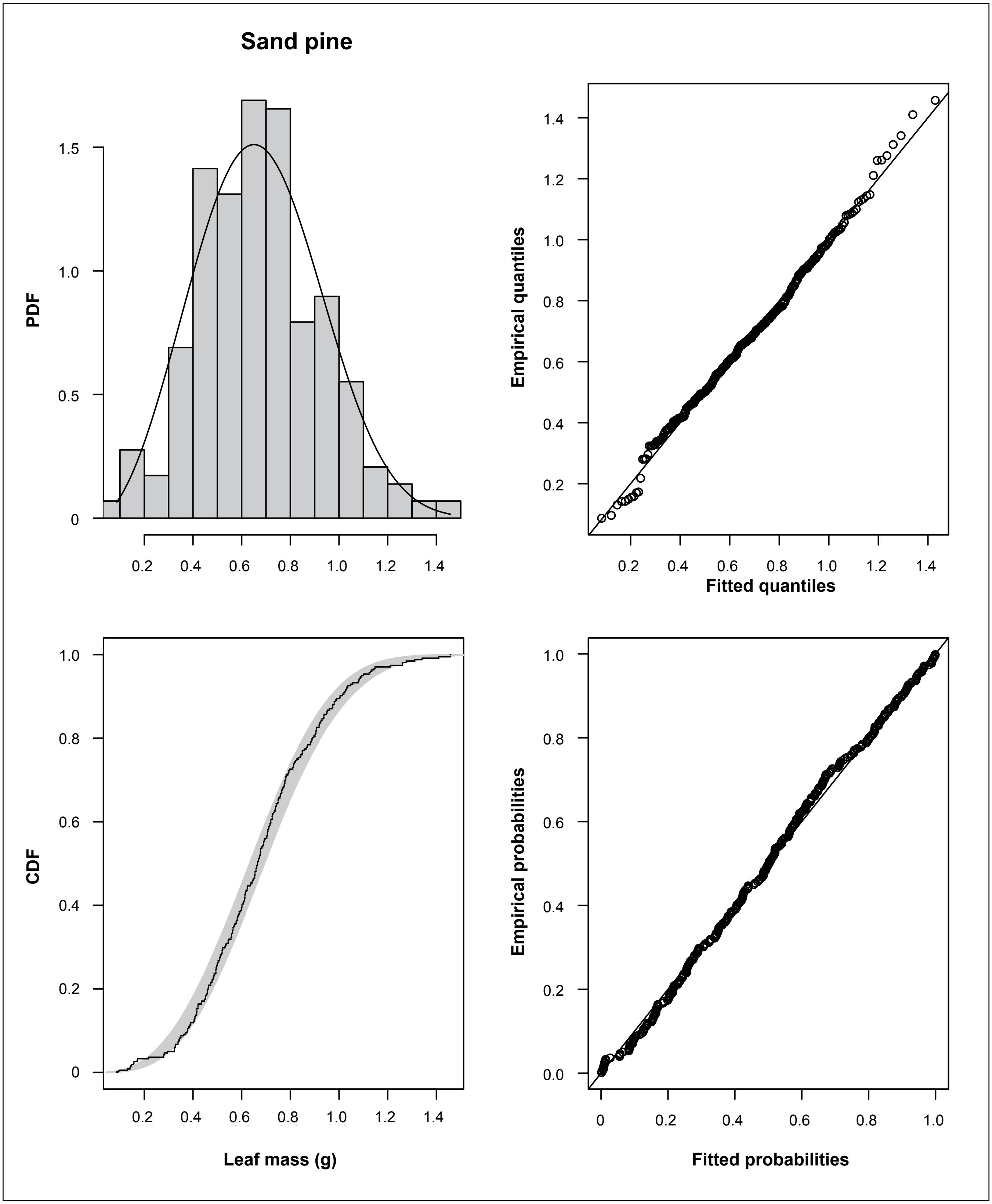

Figure 10—Continued.

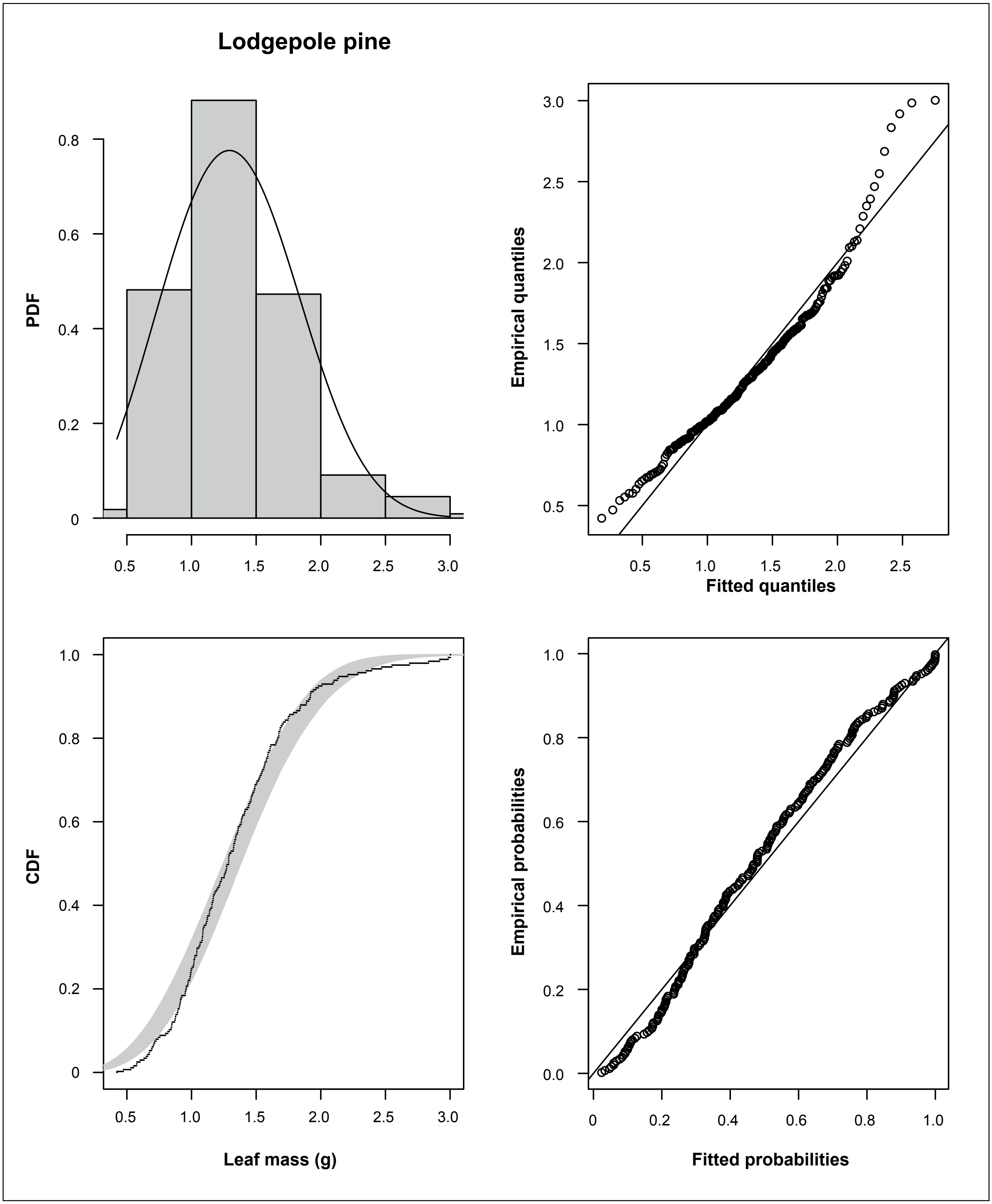

Figure 10—Continued.

This publication is available online at www.fs.fed.us/psw/.

Pacific Southwest Research Station
800 Buchanan Street
Albany, CA 94710

Official Business
Penalty for Private Use, $300